

Universität Stuttgart

**Auslandsorientierter Studiengang
Wasserwirtschaft
Master of Science Program
Water Resources Engineering and
Management - WAREM**

Master's Thesis:

**Analysis of climatic and stochastic variability
when using synthetic precipitation time series
in urban drainage modelling**

submitted by :

Jennifer Löfvendahl

Date : **November 24, 2013**

Supervisor : **Dr.-Ing. Ulrich Dittmer**

Institut für Siedlungswasserbau, Wassergüte- und Abfallwirtschaft
Lehrstuhl für Siedlungsentwässerung
Prof. Dr.-Ing. Martin Kranert
Bandtäle 2
D-70569 Stuttgart (Büsnau)

Preface

This Master's thesis has been carried out at the department of Sanitary Engineering, Water Quality and Solid Waste Management (ISWA) at the University of Stuttgart, Germany. The Master's thesis is the final examination of the double degree exchange between the Master programs Infrastructure and Environmental Engineering at Chalmers University of Technology and Water Resources and Engineering Management (WAREM) at the University of Stuttgart, and will result in a double Master's diploma.

First of all, I would like to thank my supervisors Dr.-Ing. Ulrich Dittmer and Dipl.-Ing. David Bendel at ISWA and Dr.-Ing. Ferdinand Beck at IWS (Institute for Modelling Hydraulic and Environmental Systems) at the University of Stuttgart. Your support, engagement and knowledge in this project have been very valuable to me.

I would also like to thank all the involved persons from Chalmers University of Technology and the University of Stuttgart that have been a part of my studies during this exchange. I have you to thank for the support and for also giving me the tools to succeed throughout my studies abroad.

Finally, I would like to thank my co-workers at team VA-teknik at Norconsult AB in Gothenburg. Thank you for all the help and for always making me feel like one of the team.

Gothenburg, November 2013

Jennifer Löfvendahl

Thesis Topic

The effects on urban drainage systems caused by climate change can be evaluated by modeling long-term rainfall-runoff simulations using synthetic precipitation time-series accounting for climate change. NiedSim-Klima is a precipitation generator that generates synthetic precipitation time-series that account for climate change. Synthetic precipitation time-series can be generated in a high-temporal resolution for any location in Baden-Württemberg, Germany.

When comparing the effects of climate change on precipitation patterns at different locations, it becomes clear that they are spatially heterogeneous. Furthermore, deviations are also found when comparing different precipitation realizations at one location. There are two sources that explain the variability at one location between different realizations:

1. The climatic effect, which is characterized by the resampling of the circulation pattern sequence from the climatic model ECHAM5,
2. The stochastic effect, which is obtained in the generation and in the optimization algorithms.

Additionally, in a previous study it was found that small differences in precipitation characteristics can have a great impact on overflow patterns. Similar to the situation described above, those impacts at one location are due to the variability of different synthetic precipitation realizations.

Consequently, the aim of this thesis is to present a methodology of how to determine the variability in both the precipitation generation and in the overflow characteristics due to the stochastic and climatic effect.

Climate change is an additional contributor to variability in the synthetic precipitation time-series due to the deviations within the global climate model ECHAM5, and the interpolated parameters describing the future precipitation in the optimization algorithm. As a second aim of this thesis, an assessment of the variability on precipitation patterns and overflow parameters due to climate change will be carried out.

Abstract

A method to determine the climatic- and stochastic variability present in the generation of synthetic precipitation time-series with the stochastic precipitation generator NiedSim-Klima has been carried out in this project. The project consists of two parts; *i*) determining the variability in the synthetic precipitation; and, *ii*) determining the variability in the overflow parameters. Synthetic precipitation time-series for the Holzgerlingen station in Baden-Württemberg for the time periods 1981-90 (NSK1990) and 2041-50 (NSK2050) have been generated with and without resampling of the circulation pattern sequence (CP). Ten realizations were chosen in order to determine the variability. The time-series generated without CP-resampling includes only the stochastic effect while the time-series generated with the CP-resampling includes both the stochastic- and climatic effect. The comparison of the two will yield the part of the variability that is due to the climatic effect.

The long-term averages of the precipitation and overflow parameters have been investigated in order to determine the variability between different realizations. The precipitation parameters were obtained from time-series analysis and the overflow parameters from a long-term simulation with the urban drainage model KOSIM. The parameters were analyzed using three different methods: box-and-whisker plot analysis, frequency distribution, and scatter plot analysis.

The results from the box-and-whisker plot analysis show an increase in variability due to the climatic effect for all parameters for the time period NSK1990. Thus, the variability due to the stochastic- and climatic effect can be determined. The variability analysis through the frequency distribution for the precipitation show unexpected results. The variability decreased for the highest daily precipitation intensities due to the CP-resampling. An increase in variability for all intensities was expected. The scatter plot analysis for the correlation between the yearly overflow volume and the overflow duration showed an increase in variability due to the CP-resampling for both the past and the future. However, only a visual interpretation was performed. More mathematically-correct analysis would be suggested for future investigations. The variability within the precipitation and overflow events, instead of the long-term averages, would also be suggested for the future. Then, the variability within the precipitation events causing an overflow event can be determined.

Table of Contents

Preface.....	II
Thesis Topic.....	III
Abstract.....	IV
Table of Contents.....	V
List of Abbreviations.....	VII
1 Introduction.....	1
2 Theory.....	3
2.1 The urban water cycle.....	3
2.2 The hydrological conditions in Baden-Württemberg.....	5
2.3 Expected impacts on precipitation in Baden-Württemberg due to climate change.....	8
2.4 Expected impacts on overflow patterns in Baden-Württemberg due to climate change.....	10
3 Methodology.....	11
3.1 Used precipitation time-series.....	12
3.1.1 The precipitation generator NiedSim.....	14
3.1.2 The precipitation generator NiedSim-Klima.....	16
3.1.3 Sources of variability in the precipitation generation process.....	17
3.2 Characteristics of the used Combined Sewer System.....	19
3.3 Variability in the synthetic precipitation data.....	21
3.3.1 Box-and-whisker plots.....	22
3.3.2 Frequency distribution.....	25
3.3.3 Scatter plot.....	27
3.4 Variability in the CSO overflow characteristics.....	27
3.4.1 Box-and-whisker plots.....	28
3.4.2 Frequency distribution.....	29
3.4.3 Scatter plot.....	30
4 Results.....	31
4.1 Variability in the synthetic precipitation data.....	31
4.1.1 Box-and-whisker plots.....	31

4.1.2	Frequency distribution.....	39
4.1.3	Summary	44
4.2	Variability in the overflow characteristics	44
4.2.1	Box-and-whisker plots.....	45
4.2.2	Scatter plot.....	49
4.3	Summary.....	51
5	Conclusion and outlook	52
5.1	Box-and-whisker plot analysis and number of realizations.....	52
5.2	Frequency distribution	52
5.3	Scatter plot.....	53
5.4	Climate change	53
5.5	Outlook.....	53
6	Bibliography.....	55
6.1	Figures	56
6.2	Tables	57
7	Annex.....	58
7.1	Constructing box-and-whisker plots in Excel.....	58

List of Abbreviations

CP	Circulation Pattern for weather type classification
CSO	Combined sewer overflow
CSS	Combined sewer system
DOF	Degree of Fulfillment (of Fuzzy Logic rule)
DWD	Deutscher Wetterdienst, German meteorological service
ECHAM5	Global Circulation Model developed by the Max-Planck Institute, Hamburg, Germany
GCM	Global Circulation Model
IPCC	Intergovernmental Panel on Climate Change of the UN
KOSIM	KOntinuierliches Langzeit- SIMulationsmodell, hydraulic model for sewage system simulations
MSLP	Mean Sea Level Pressure
NCAR	National Center for Atmospheric Research of the United States
NCEP	National Centers for Environmental Prediction of the United States
NSK1990	Precipitation time-series generated with NiedSim-Klima for the time period 1981-1990
NSK2050	Precipitation time-series generated with NiedSim-Klima for the time period 2041-2050
RCM	Regional Climate Model

1 Introduction

As urban areas grow, the need for safe stormwater management becomes increasingly important. Infrastructure as well as public and private developments change the landscape and the localized stormwater runoff. In Germany, urban areas are mainly drained by combined sewer systems (CSS), whose essential features are that it transports both waste- and stormwater in the same pipe, and that the combined flow eventually terminates at the wastewater treatment plant (Butler & Davies, 2010). However, the pipes are not designed to carry the highest combined flow-rates, which normally occur during heavy storm events. Therefore, it is necessary for some of the flow to be discharged into a watercourse, at a combined sewer overflow (CSO). During an overflow event, a substantial amount of pollution is discharged into the aquatic environment.

The CSO activity in a combined sewer system can be evaluated and controlled by using numerical computer models. By simulating one or multiple rain events over a catchment area, the discharge of the combined flow into the watercourse can be calculated. In the design and planning of sewer systems, numerical models are being utilized. As climate change may alter precipitation patterns, there are reasons to believe that this will also affect CSO activity. Therefore, in the evaluation and planning of sewer systems, the effects of climate change should to be considered.

One way to investigate the impacts of climate change on urban drainage systems is to use synthetic precipitation time-series of the past and future in long-term urban drainage simulations. To generate synthetic precipitation time-series, a precipitation generator is needed. NiedSim-Klima is one such example, which is based on the stochastic precipitation generator NiedSim (Bárdossy, 1998), and is able to generate synthetic precipitation time-series in a high-temporal resolution for any location in Baden-Württemberg, Germany (Beck & Bárdossy, 2011). The NiedSim-Klima precipitation generator has been modified to account for climate change, and uses forecasts of air pressure at sea level and the mean air temperature from the global climate model (GCM) ECHAM5, as well as historical observations in order to generate precipitation time-series for the past and the future.

When comparing different generation realizations at one location, deviations between the realizations are found. This is due to the heterogeneous behavior of precipitation which is a result of the natural variability in the climate. The natural variability is present in all time-scales as well as in all spatial scales (Ghil, 2002). In the development of a precipitation generator, it is desired to account for the natural variability in the precipitation time-series.

In NiedSim-Klima, two sources explain the variability in the generation of precipitation time-series:

1. The climatic effect, which is characterized by the resampling of the circulation pattern sequence from the global climate model ECHAM5,
2. The stochastic effect, which is obtained in the generation and optimization algorithms.

From the ECHAM5 model, the circulation pattern (CP) sequence and the mean temperature are obtained. The CP describes the mean sea level pressure fields over Europe and the northern Atlantic Ocean for each day. Depending on the CP and the temperature for each day, a certain precipitation response is obtained, which, ultimately with randomly-generated numbers that correspond to each hour of the day, prepare an initial time-series. Afterwards, a Simulated Annealing algorithm optimizes the time-series depending on the precipitation statistics. The climatic effect is due to the resampling of the CP-sequence, while the stochastic effect is due to the setup of the initial time-series and the optimization algorithm.

Climate change also contributes to the variability in the precipitation generation due to the deviations within the global climate model ECHAM5, and the extrapolated parameters describing the future precipitation in the optimization algorithm.

When investigating the effects of climate change on urban drainage using synthetic precipitation time-series, previous studies show that relatively small changes in the precipitation patterns can have a huge impact on the overflow characteristics. These impacts result from the variability within the synthetic precipitation. Therefore, it is important to be aware of the variability within the precipitation time-series and its effect on the overflow parameters when designing and controlling urban drainage systems for future conditions.

Thus, this study aims to present a method in order to determine the variability in the precipitation generation and in the overflow characteristics due to the climatic- and stochastic effect.

The effect of climate change on the variability and the precipitation- and overflow characteristics will be carried out as a second objective in this study.

2 Theory

A basic understanding of the urban water cycle and the impacts of climate change are needed in order to understand and assess the variability within the synthetic precipitation and the overflow characteristics. An explanation of the urban water cycle and the previous research on climate change impacts in Baden-Württemberg will be provided in the following chapters.

2.1 The urban water cycle

When rain falls on a natural surface, three different processes occur (Butler & Davies, 2010):

- *Evapotranspiration*, a process through which water is absorbed by plants and may also refer to water returning to the atmosphere;
- *Infiltration*, by which rainwater permeates the natural ground cover; and,
- *runoff*, whereby the rainwater flows over the natural ground cover.

These three processes are presented in Figure 2.1. The relative magnitude of each process depends on the ground cover and varies with time during the storm event. As the ground becomes increasingly saturated, the surface runoff will increase, and both the groundwater and the surface runoff will be discharged in rivers or other watercourses. The groundwater contributes to the rivers or streams base flow, while the surface runoff increases the flow in the watercourse.

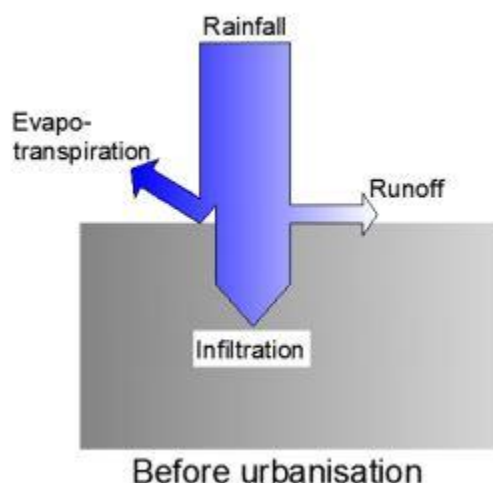


Figure 2.1. Magnitude of the processes occurring when rain falls on a natural surface (Butler & Davies, 2010). Modified by Erika Nilsson

Urbanization leads to changes in the natural landscape by artificial surface materials covering natural surfaces (Butler & Davies, 2010). The artificial surfaces are often impervious and obstruct the rainwater from infiltrating into the ground. Thus, the surface runoff will increase. The evapotranspiration will decrease due to the lack of vegetation and availability of rainwater detention areas. The processes and their relative magnitude as a result of urbanization are explained in Figure 2.2. Due to the increased amount of surface runoff, the total volume of water reaching the rivers and streams will increase. The stormwater also travels faster on artificial surfaces, leading to higher peak flows. Consequently, the risk of flooding near rivers and other watercourses will increase.

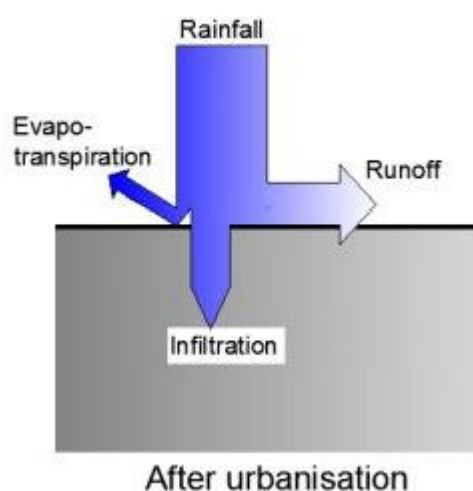


Figure 2.2. Magnitude of the processes occurring when rain falls on an urban surface (Butler & Davies, 2010). Modified by Erika Nilsson

In developed urban areas, urban drainage systems are required due to human interactions with the natural water cycle (Butler & Davies, 2010). Primarily, these interactions are: the discharge of water resources and the obstruction of rainwater, which results from impervious artificial surfaces. These interactions lead to two types of water that requires drainage: wastewater from water usage, and stormwater generated from surface runoff. Without urban drainage systems, these flows threaten clean and safe living environments, as well as increase the risk of flooding and further property damage.

Urban areas often depend on artificial systems consisting of pipes and structures that collect and release waste- and stormwater (Butler & Davies, 2010). In Germany, 70 % of these systems are combined sewer systems (CSS). The essential feature of a CSS is that it transports both waste- and stormwater in the same pipe to the wastewater treatment plant (WWTP) before released into the recipient.

However, combined sewer systems are not designed to sufficiently manage the highest stormwater peak flows, as it is not economically-feasible to construct such systems nor to have the capacity to treat the highest flow at WWTP (Butler & Davies, 2010). Therefore, the need of combined sewer overflows (CSOs) is an essential feature in combined sewer systems. The CSOs are placed downstream in a catchment area and are designed to carry a continuation flow to the WWTP. When the continuation flow is exceeded, an overflow event occurs in the CSO.

Overflow events can lead to impaired water quality and therefore, in order to minimize these occurrences, drainage systems should be properly designed, controlled, and analyzed. The design of sewer systems is a balance between cost and potential damage. Urban drainage systems are long-term investments with lifespans of 50 to 100 years, according to the German standard ATV-A 128E (German Association for the Water Environment, 1992). Consequently, sewer systems built today need to be safe even for future climatic conditions. Thus, it is of great importance to understand and assess the changes in climate.

2.2 The hydrological conditions in Baden-Württemberg

Baden-Württemberg is one of Germany's 16 federal states (Bundesländer) and is situated in southeast Germany, see Figure 2.3. As part of Central Europe, Baden-Württemberg experiences highly-variable weather conditions and precipitation occurrences (Beck, 2012). In general, the highest monthly precipitation sum is in June while the lowest is in February. However, precipitation can occur at any time during the year. The yearly precipitation sum for Baden-Württemberg is between 550 to 850 mm per year.



Figure 2.3. Baden-Württemberg is situated in southeast Germany (Baden-Württemberg Studyguide, 2013)

Precipitation is the result of condensation of water vapor in the atmosphere due to the circulation of warm and cold air masses. Air circulation results primarily from two sources: air temperature and Earth's rotation (State Climate Office of North Carolina, 2013). On the global scale, due to different exposure angles to the sun, elevated warm air and sunken cold air results in a high-pressure gradient between the Equator and the North- and South Poles (Wischet & Endlicher, 2008 through Beck, 2012). This pressure gradient induces a strong compensation movement in the northern hemisphere from south to north. Additionally, air movement induced by Earth's rotation, known as the Coriolis Effect, results in a zonal west wind in the atmosphere, which can obstruct the exchanges of air masses between the southern and the northern latitudes.

However, this zonal west wind can be affected by the pressure gradient and destabilize, allowing an exchange between the south and the north. In the west wind field, waves are formed, which move in a south-easterly direction. The exchange between warm and cold air is governed by the direction of these waves. If the waves peak to the north, warm air can move to the north, and where the wave peak to the south, cold air can move south. At the border between cold and warm air, precipitation will occur.

The west wind eventually stabilizes and the cycle starts anew. However, sometimes a phenomenon known as "blocking action" occurs. In the end of the undulating phase, cold air can be cut off from the interface between the warm and the cold air, and move southeastwards.

This can block the west wind until the gradient increases enough and the main western flow direction can be re-established. The blocking action can be caused by warm air from the southern altitudes as well.

The global atmospheric circulation governs the local atmospheric conditions in Baden-Württemberg. Due to the zonal west wind, the main flow direction in Baden-Württemberg is from west-southwest (Beck, 2012). Thus, the weather conditions are mainly determined by the energy and moisture from the Atlantic Ocean. Generally the atmospheric cycles change in irregular intervals over several days. However, the blocking actions, described in the paragraph above, can last up to several weeks. The average weather conditions are governed by the west-wind field over Europe. As mentioned above, if the wave embedded in the field, moves north, warm air can enter and the conditions are warm and humid. If the wave moves south, colder winds from the northeast creates cooler conditions. During blocking situations, dry conditions can establish as the heat and moisture fluxes are cut off. Thus, longer dry periods are always caused by blocking situations.

The characteristics of the weather conditions in Central Europe, and thus, Baden-Württemberg, are also triggered by circulation patterns in lower levels. The area over the West Atlantic where the gradient between warm and cold air masses is the most pronounced is called the polar front. The waves embedded in the west wind fields affect the stability of the polar front which forms smaller waves. These smaller waves, referred to as cyclonic depressions, start to circulate and move southeastwards over Europe. Depending on where the cyclonic depressions are formed, their pathway determines the weather conditions in Europe. Thus, the weather conditions in Baden-Württemberg are highly affected by the cyclonic depressions.

The precipitation in Baden-Württemberg is mostly due to warm and cold fronts of the cyclonic depressions. Two types of precipitation occurs, advective precipitation at warm fronts and convective at cold fronts. The advective precipitation is usually not strong in intensity but generally long lasting. Convective precipitation has a higher intensity but with a shorter duration. As mentioned before, the highest monthly precipitation sum is in June and this is due to an enhanced convection because of high solar radiation.

2.3 Expected impacts on precipitation in Baden-Württemberg due to climate change

According to the fourth assessment report by the Intergovernmental Panel on Climate Change (IPCC), the climate is most likely changing due to anthropological effects (IPCC, 2007). An increase in the emissions of greenhouse gases is causing an increase in the global mean temperature. Studies also show that climate change does not only affect the atmospheric temperature, but also atmospheric circulation patterns (Auer et al., 2007; Beck, 2012).

Moreover, the global water-cycle is sensitive to changes in the global mean temperature (Beck, 2012). The amount of water within the hydrosphere is constant and an increased temperature enhances the evapotranspiration and the air's moisture content. If more water is present in the atmosphere it has to fall somewhere in order to complete the mass balance. However, a higher global precipitation volume does not inform the spatial-temporal distribution of the precipitation (Beck, 2012). The yearly precipitation amount may increase but rain events may be fewer and more intense with a higher seasonality. This will increase the risk of flooding as well as the stress on the water resources. The effect in the precipitation patterns will look different in different parts of the world.

In Baden-Württemberg, the trend in daily precipitation patterns has been analyzed in previous studies. Hundecha & Bárdossy (2005) studied records from 632 precipitation stations between the years 1958 to 2001 (Beck, 2012). Most of the precipitation parameters studied, including the extreme events, indicated an increasing trend. There is a pronounced increase in precipitation in the winter months and in the summer months there is a slight decrease. The same results are obtained from predictions using global circulation models for Central Europe.

Extreme events on different temporal scales are caused by different events (Beck, 2012). Daily precipitation extremes are caused by cyclonic depressions originating from the Atlantic Ocean as described in Chapter 2.2. Extreme events on the hourly scale are mainly caused by convective precipitation. Thus, daily extreme precipitation cannot predict the effect of climate change on the hourly scale.

One way to predict future climate conditions is to extrapolate observed trend-signals (Beck, 2012). In Figure 2.4 below, the scaling properties for the five highest extremes have been evaluated. As extreme events on different time scales are caused by different process, scaling is a sufficient method to display the statistical properties of precipitation. As seen in the figure, a trend towards higher precipitation intensities for shorter time intervals is present.

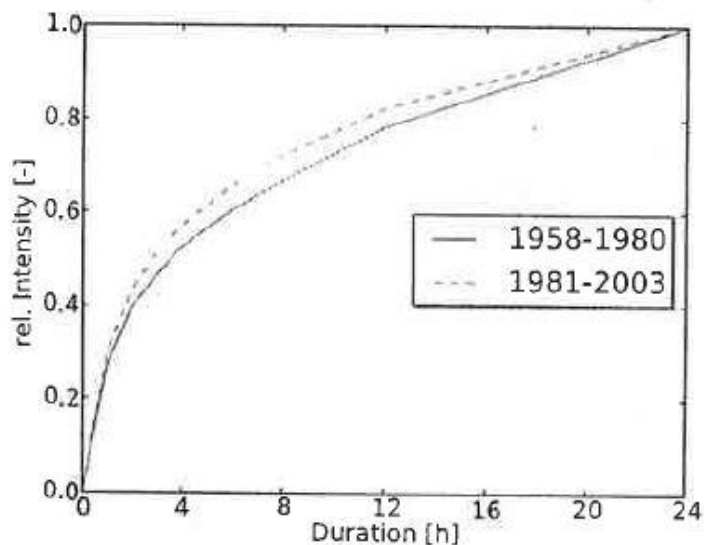


Figure 2.4. Scaling properties for the five highest extremes for the time periods 1958-1980 and 1981-2003 (Beck, 2012)

Extrapolation of the trend for future conditions shows an even more pronounced trend on shorter time intervals, see Figure 2.5 (Bendel et. al, 2013). Future conditions, represented by the red data line show that approximately 60 % of the daily precipitation will fall within one hour compared to the past conditions, where 35 % of the daily precipitation fell within one hour. Thus, a trend towards higher intensities on hourly scale due to climate change is present.

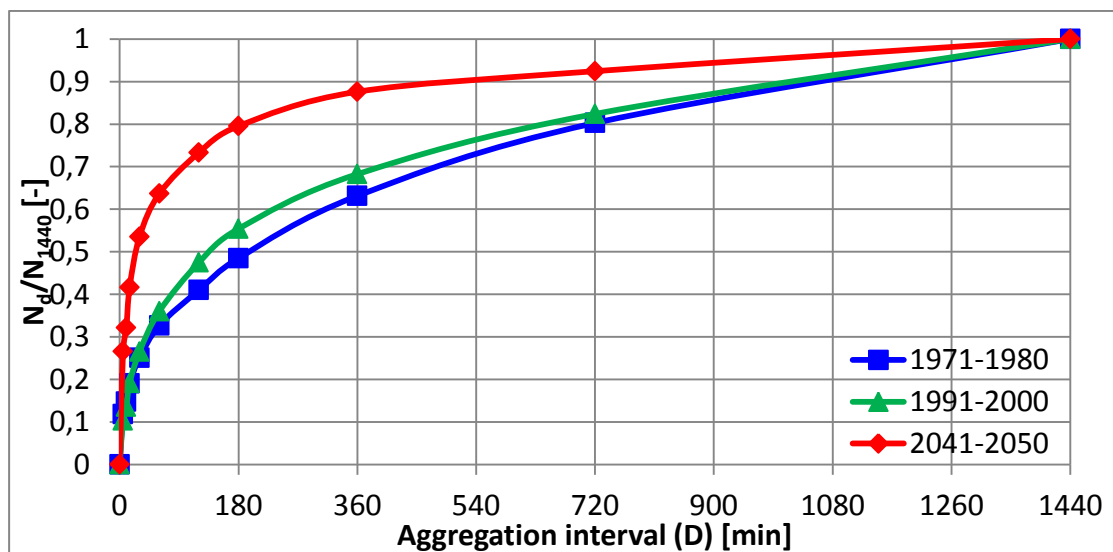


Figure 2.5. Scaling properties for precipitation intensities for the past and future (Bendel et al, 2013)

The results shown in Figure 2.4 and 2.5 support the thesis of Trenberth (1999), which hypothesized that the precipitation on shorter time scales will be more intense due to climate change (Beck, 2012).

2.4 Expected impacts on overflow patterns in Baden-Württemberg due to climate change

The changes in precipitation patterns will most likely affect the overflow patterns at the CSOs. In a study carried out by Bendel, Beck & Dittmer (2013), the impacts of climate change on combined sewer overflows were investigated. Synthetic precipitation time-series generated by NiedSim-Klima was used as input in long-term simulations with the hydrological model KOSIM. The overflow parameters from seven stations in Baden-Württemberg were compared using data from past and future simulations.

Although the annual precipitation sum increased, the results showed a decrease in the yearly net flow into the system (Bendel et al., 2013). An explanation for this outcome may be that the precipitation events are shorter and occur more often. As a result, the runoff decreases due to increased evapotranspiration and infiltration. Moreover, the overflow volume decreased while the frequency of overflow events increases.

In the study by Bendel et al. (2013), the need to investigate the variability within the synthetic precipitation was found. Thus, the study by Bendel et al. (2013) is the main reason and background for investigating the variability in the precipitation generation and in the overflow characteristics in this project.

3 Methodology

The aim of this project is to present a strategy to determine the variability in the synthetic precipitation and overflow parameters at one location, due to the climatic- and stochastic effect. The project has been divided into two parts as the variability within the two fields have been examined separately. In Figure 3.1 below, the workflow used in this project is presented.

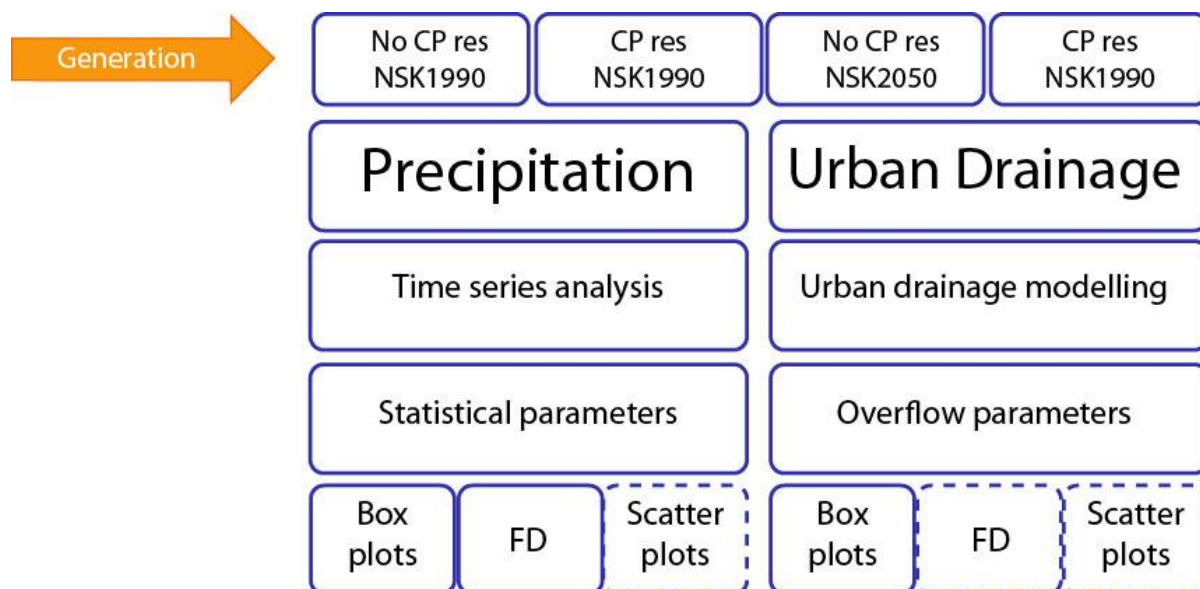


Figure 3.1. Workflow (Löfvendahl, 2013)

The analysis tools represented in the bottom of the figure, namely box-and-whisker plot analysis, frequency distribution analysis and a correlation analysis visualized in a scatter plot, have been used for both the precipitation and the urban drainage part of this thesis. These methods represent the strategy to determine the variability and will be explained more thoroughly in chapters 3.3 and 3.4.

To be able to determine the variability due to the climatic- and stochastic effect, a three-stage approach has been used in the generation of the synthetic precipitation time-series:

1. Generation of precipitation time-series at one location with the same circulation pattern sequence (CP) without resampling (**No CP res**)
2. Generation of precipitation time-series at one location each with a new circulation pattern sequence (CP) with resampling (**CP res**)
3. Comparison of stages one and two

The first stage will only include the variability due to the stochastic effect, while stage two will include the variability due to both the stochastic- and climatic effect.

The comparison of stage one and two will yield the part of the variability that is due to the climatic effect. The three-stage approach is illustrated in Figure 3.2, where the stochastic effect is represented by the variability in the **No CP res**, and the climatic effect is represented by the part of the variability in the **CP res** that is not due to the stochastic effect.

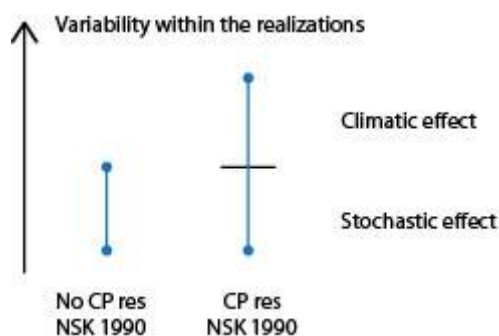


Figure 3.2. Illustration of the climatic- and stochastic variability (Löfvendahl, 2013)

In Figure 3.1, the precipitation time-series is represented by the boxes in the top of the figure. The generation of the precipitation time-series will be presented more thoroughly in Chapter 3.1.

To be able to determine the variability in the synthetic precipitation at one location, a time-series analysis has been carried out in order to obtain the long-term averages for the selected precipitation parameters. The chosen precipitation parameters will also be presented in Chapter 3.1.

Long-term averages have also been determined for the overflow parameters. Long-term simulations with the urban drainage model KOSIM have been conducted. The chosen parameters and the description of the model are presented in Chapter 3.2.

3.1 Used precipitation time-series

The synthetic precipitation time-series was generated for one location, namely Holzgerlingen, southwest of Stuttgart in Baden-Württemberg, Germany. Consistent with the three-stage approach, the time-series were generated according to stage one and two, as noted above.

Two time periods have been used for the generation of the time-series: one representing the past NSK1990 (1981-1990) and the other one representing the future, NSK2050 (2041-2050). Generation of past and future data is necessary in order to determine the influence in the variability due to climate change, which is a secondary objective of this project.

Comparing past and future data with identical initial properties, yields the variability due to climate change.

Consequently, there are four different precipitation time-series to analyze, each with the length of 10 years:

- Generation with *the same Circulation Pattern sequence* for the time period NSK1990 – **No CP res NSK1990**
- Generation with *a new Circulation Pattern sequence* for the time period NSK1990 – **CP res NSK1990**
- Generation with *the same Circulation Pattern sequence* for the time period NSK2050 – **No CP res NSK2050**
- Generation with *a new Circulation Pattern sequence* for the time period NSK2050 – **CP res NSK2050**

Each precipitation time-series has been generated ten times, i.g. ten realizations, to be able to determine the variability in the precipitation generation. The number of realizations is crucial as precipitation is highly variable and it is important that the dry spells and the extremely wet years are represented in the time-series in each generation in order for the analysis to be statistically correct.

The temporal resolutions analyzed for the precipitation time-series are the hourly and daily precipitation intensities. Figure 3.3 below illustrates the generation structure of the data used in this study. The branch under the **No CP res NSK1990** is the same for all four time-series.

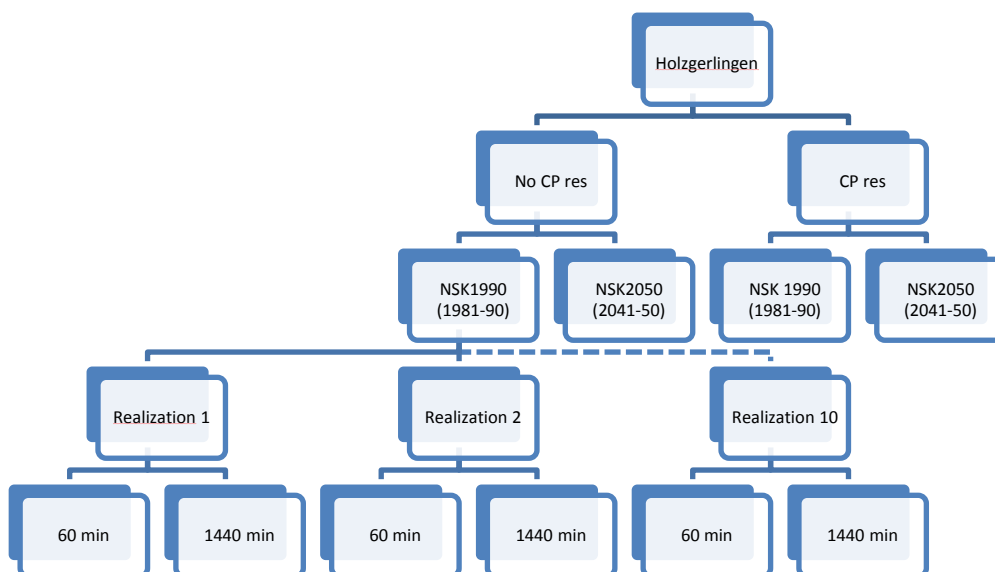


Figure 3.3. Generation scheme of the synthetic precipitation time-series (Löfvendahl, 2013)

The time-series analyzed in this study are generated by the stochastic precipitation generator, NiedSim-Klima, which is based on the precipitation generator NiedSim. The main difference behind the two generators is that NiedSim-Klima also accounts for climate change (Beck & Bardossy, 2011). To be able to account for climate change, NiedSim-Klima uses forecasts from the ECHAM5 model in order to describe the future climate.

Thus, in NiedSim-Klima, a CP-Temperature classification is used as input in the setup of the initial time-series. It is mainly the method used to setup the initial time-series that differs between the two generators. NiedSim-Klima uses forecasts from ECHAM5 to classify CP-temperature classes with a certain precipitation response, while NiedSim uses collected rainfall data for the setup of the initial time-series. Other than the setup of the initial time-series, the two generators originate from the same approach. Therefore, the theory behind NiedSim is also presented in this chapter as it enables the understanding of the NiedSim-Klima application.

3.1.1 The precipitation generator NiedSim

NiedSim is a stochastic precipitation generator, which is able to generate precipitation data in a high-temporal resolution, for any location in Baden-Württemberg, Germany (Beck, 2012). NiedSim has been utilized since the year 2000 and is mainly used by federal states in southern Germany for the generation of synthetic precipitation data.

NiedSim uses a data-driven approach to generate precipitation time-series (Beck, 2012). This method makes as few assumptions as possible and uses collected rainfall data to describe the statistical appearance of precipitation in the area. The only conceptual specification in NiedSim is the theoretical distribution of precipitation values. Instead of directly using rainfall values, the statistical parameters from surrounding rainfall gauges are interpolated in the NiedSim generator. The statistical parameters are stored in a data-base, and according to these parameters, a stochastic simulation is carried out.

Initially, a time-series of hourly values with the correct intensity distribution is configured (Beck, 2012). However, the temporal sequence of values differs from real precipitation characteristics in the following statistics: autocorrelation, daily rainfall frequency and scaling. The autocorrelation is a measure of the degree of similarity between a time-series and a lagged version of itself. A positive autocorrelation describes the persistence in a rain event. For example, if it rains in the present time-step, the likelihood of rain in the next time step, is high (Beck, 2012).

As mentioned in chapter 2.3, scaling is a measure of how statistical properties change when the data is aggregated over longer time intervals. The daily- and hourly extreme values for a certain location depend on different climatic processes and thus, the hourly extreme precipitation intensity can be higher than the daily extreme precipitation intensity. Therefore, the extreme precipitation aggregated over a 24h-time-period shows a concave function between 1 and 24h.

In order to determine the correct temporal sequence, the time-series is optimized by an objective function, where the statistical characteristics of the time-series are compared with the target parameters derived from real world observations (Beck, 2012). If the synthetic time-series perfectly fulfills the target parameters, the objective function, $O(Z)$, is zero. The objective function is minimized by using a Simulated Annealing algorithm that repeatedly tries to swap two arbitrarily chosen rainfall values in order to obtain the correct temporal sequence, see process scheme in Figure 3.4. If the swap improves the objective function, the changed time-series is kept. However, if the swap does not improve the objective function, the changed time-series is kept with a certain probability. This is necessary to not end up in a local minimum. The probability of accepting an incorrect swap decreases as the algorithm proceeds. The algorithm stops when no further improvement of the time-series is possible. In order to dis-aggregate five-minute rainfall values from the hourly values, a similar Simulated Annealing optimization scheme is used.

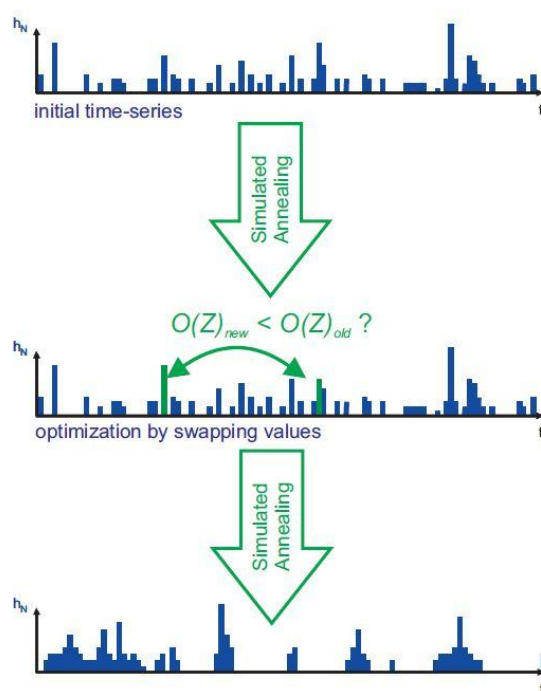


Figure 3.4. Optimization process by the Simulated annealing algorithm (Beck, 2012)

3.1.2 The precipitation generator NiedSim-Klima

NiedSim-Klima is based on the stochastic precipitation generator NiedSim (Beck & Bárdossy, 2011). Instead of directly using precipitation statistics from rain-gauges, NiedSim-Klima uses forecasts of air pressure at sea level and the mean air temperature from the global circulation model ECHAM5 to estimate indirectly the future precipitation.

Similar to NiedSim, an initial time-series of hourly precipitation is set-up, which is based on a classification of a number of atmospheric circulation patterns (CP) and their respective precipitation response. The mean sea level pressure (MSLP) field over Europe and the northern Atlantic Ocean is based on the re-analysis of records of more than 50 years of global analyses of atmospheric fields. The re-analysis is carried out by the National Centers for Environmental Prediction (NCEP) and the National Centre for Atmospheric Research (NCAR). A more thorough description of the CP-classification can be found in Bárdossy et al. (1995).

Based on historical observations for the time period 1991-2003, empirical precipitation distributions are calculated for each CP (Beck, 2013). Assuming that the precipitation distribution for each CP stays the same in the future, the precipitation probability and the probability of intense precipitation can be calculated. Intense precipitation is assumed to be more than 1 mm per hour.

The CP classes are subdivided according to the mean temperature, which is due to the low probability of precipitation at high mean temperatures, but when precipitation does occur, there is a high probability that the rain event is intense.

For each day, the predicted mean sea level pressure field and the predicted temperature from the ECHAM5 model are compared with the CP-classification matrix from the CP classification. The number of CPs is set to 12 in the classification. The CP with the highest resemblance, degree of fulfillment, to the MSLP-field from the ECHAM5 model is chosen as the daily CP. A time-series with daily CPs are set-up for the chosen time period. Each CP in the time-series is subdivided by temperature. Depending on the CP-Temperature class, the precipitation probability and the probability of intense rainfall are estimated for each day. Based on the precipitation response, rainfall intensities are drawn for every hour. Intensities between 0-1 mm/h are drawn from a Beta distribution and values above 1 mm/h from a Weibull distribution.

The time-series are then optimized by a similar Simulated Annealing algorithm used in NiedSim (Beck & Bárdossy, 2011). It evaluates an optimization function under certain constraints and when no improvement is possible, the algorithm stops.

The constraints used for NiedSim-Klima are additional historical parameters such as the autocorrelation on different aggregations and with different time-lags. For future, synthetic precipitation time-series, the autocorrelation does not change as it is assumed to be the same even in the future. However, other parameters are used in the optimization and have been extrapolated to resemble future conditions. The scaling behavior is extrapolated for the future and is used as a constraint in the optimization. The extreme 24h-sum is a parameter derived from the regional climate model REMO, and is also used as a constraint in the optimization. The generation scheme is illustrated in Figure 3.5.

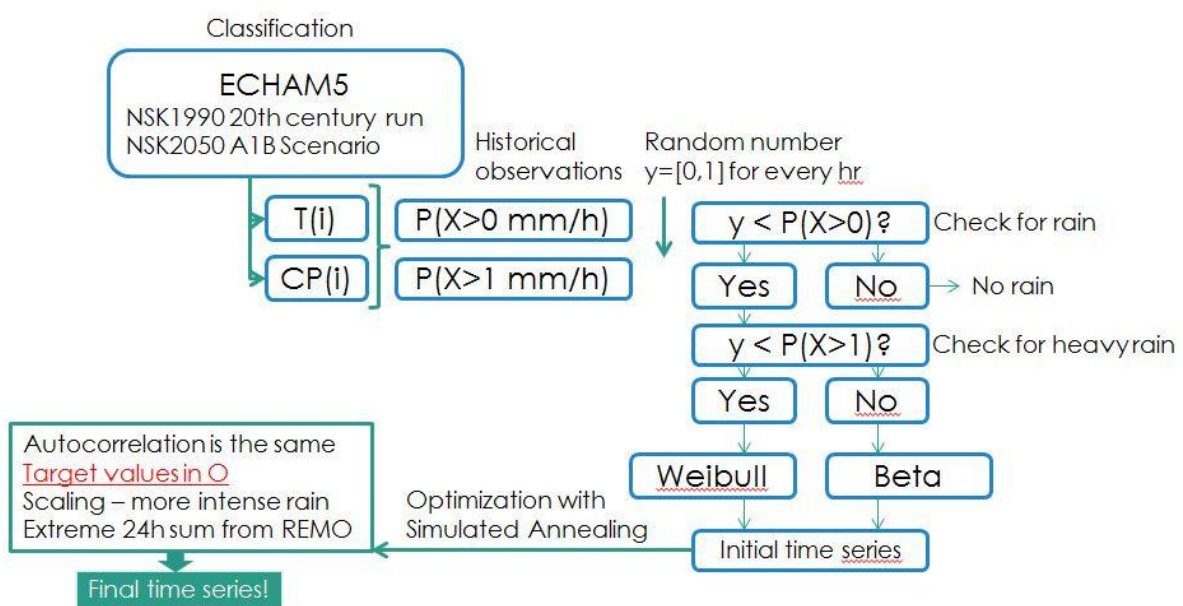


Figure 3.5. Generation scheme for NiedSim-Klima (Löfvendahl, 2013)

3.1.3 Sources of variability in the precipitation generation process

As mentioned in the Introduction, precipitation has a natural variability that is desired to be captured in the generation of synthetic precipitation time-series. In the generation of precipitation time-series with NiedSim-Klima, there are two effects responsible for the variability between different generation realizations: the stochastic- and climatic effect. In the sections below, an explanation from where these effects originate is described. Climate change is also added to the list of variability as NiedSim-Klima is modified to account for this.

Stochastic effect

The variability in the synthetic precipitation data due to the stochastic effect is a result of the generation and the Simulated Annealing algorithm. In the configuration of the initial time-series for each CP, a random number must be drawn each hour, which will contribute to a precipitation intensity and is based on the empirically derived precipitation distributions, see figure 3.5. Even in the Simulated Annealing algorithm, randomness is present due to the arbitrarily chosen values in the evaluation of the objective function. Also, the use of distributions as constraints in the objective function contributes to a stochastic variability between different generation realizations.

Climatic effect

The variability in the synthetic precipitation data due to the climatic effect is a result of the setup of the CP-temperature sequence. As described in the description of the NiedSim-Klima generator, the precipitation response for each day is dependent on the MSLP-field, which is derived from the ECHAM5 model. The probability that a certain CP follows another CP is calculated from an ECHAM5 simulation for a normal period (Beck & Bárdossy, 2013). A probability matrix, dependent on the normal simulation period of the 12+1 CPs, determines into which sequence the CPs are distributed. There are numerous combinations of possible sequences, all deriving from the same matrix with the same statistical properties. A resampling of the CP-sequence, meaning that each realization has a unique CP-sequence, is the manner in which NiedSim-Klima tries to account for the natural variability.

Climate change

Climate change is an additional source of variability in the synthetic precipitation data due to the A1B scenario simulation from the ECHAM5 model. The A1B scenario is carried out by the IPCC and is one of the developed scenarios describing the change in climate due to anthropological effects (IPCC, 2007). The scenario assumes economic- and population growth, as well as technical developments, until 2100. The assumptions predict emissions of greenhouse gases, leading to changes in the atmosphere.

Even in the generation algorithm, the climate change variability is present due to the extrapolated parameters used to describe and optimize the precipitation time-series for the future. The different CP-Temperature classes and their respective precipitation response are assumed to be the same for future conditions. This is an essential feature of the NiedSim-Klima generator. Therefore, only the sequence in which the CPs occurs will be different in the future.

3.2 Characteristics of the used Combined Sewer System

As applied to urban drainage, long-term simulations with the hydrological model KOSIM have been performed in order to obtain the long-term average values of the overflow characteristics. KOSIM is a deterministic model, thus, performing simulations with equal input values, will generate equal results. Consequently, using different precipitation time-series as input, the simulations will derive different results due to the variability within the time-series.

The purpose of an urban drainage model is to mathematically describe the transformation of a rainfall hyetograph into a surface runoff hydrograph and its hydraulic response in the pipe network (Butler & Davies, 2010). Transforming the rainfall hyetograph into a surface runoff hydrograph involves two parts. Firstly, the effective rainfall is determined by subtracting the losses due to interception, depression storage, infiltration, and evapotranspiration. Interception is characterized by the collection and retention of vegetation, while depression storage is stormwater trapped in minor depressions in the catchment surface. Infiltration and evapotranspiration are described in Chapter 2.1.

Secondly, after the losses have been accounted for, the effective rainfall is transformed into an over-land flow hydrograph by surface-routing. The process of surface-routing describes the movement of the runoff across the surface to the nearest sewer system entry. In KOSIM, the Kalinin-Miljukov-Method is used to mathematically describe this process. The sub-catchments in KOSIM are represented by linear reservoirs connected in series, where the number of cascades is set to three, and the equal storage coefficient is calculated using an overland flow time of four minutes. The CSO structures in the system with no storage are modeled as flow dividers. More information about the theory behind the model can be read in ITWH (2009).

In the simulations, a standardized virtual Combined Sewer System (CSS) was used, see Figure 3.6. The CSS-system is designed as a standard system and has been used for comparative simulation studies in Germany (Bendel et. al., 2013). The system represents a typical provincial town in Germany with 9,900 residents, two industrial polluters, and a total impervious area of 102.5 ha.

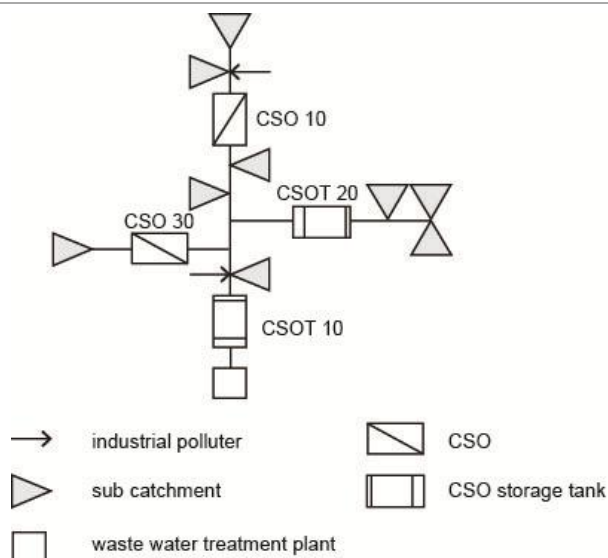


Figure 3.6. Standardized combined sewer network used in the simulations (Bendel et. al, 2013)

In the CSS network, four CSO structures are used. Two are regular CSOs (CSO10 and CSO30) with a continuation flow of 14.4 l/(s·ha) and 14.9 l/(s·ha), respectively. The remaining two are CSOs with a storage tank to retain the flow before releasing it into the watercourse. The continuation flow for the CSOT10 is 1.25 l/(s·ha) and for the CSOT20 is 1.23 l/(s·ha). The tank volumes are calculated according to the German technical standards ATV-A 128E (German Association for the Water Environment, 1992). The tank volumes were adjusted to the local annual precipitation of the past, resulting in tank volumes of 1012 m³ for CSOT10 and 180 m³ for CSOT20. When the continuation flow is exceeded, the flow is retained in the storage tanks and an overflow occurs when the tank volume is full. CSOT10 is placed downstream the CSS, see Figure 3.6. Therefore, it is the CSO structure with the highest inflow and overflow volume, about 70 % of the total yearly amount.

For future conditions, urbanization will most likely lead to changes in the urban drainage systems. As more infrastructure is developed, higher demands regarding detention within the developed area, as well as sustainable urban drainage systems (SUDS), will be necessary. Thus, different conditions and design principles for urban drainage systems is expected for the future. However, the variability and the effect of climate change are, as investigated in this study, within the synthetic precipitation time-series and its response to the overflow parameters. Thus, no changes in the setup of the model have been made due to the different time periods. The attributes in the model are therefore the same for the past and the future conditions.

For each simulation, the long-term average parameters regarding inflow and overflow have been used in the variability analysis. The parameters describing the overflow of pollutants have not been considered in this study.

The variability analysis of the selected overflow parameters will be described in Chapter 3.4. Firstly, the variability in the synthetic precipitation time-series will be explained.

3.3 Variability in the synthetic precipitation data

In the first part, the variability within the synthetic precipitation time-series has been examined. The time-series from each of the four generations have been analyzed and the long-term averages of the statistical parameters have been calculated. The variability in each parameter within the ten realizations has been determined by using box-and-whisker plots. The variability within the frequency distribution has also been analyzed. An objective at the beginning of this project was to determine the variability in the correlation between different precipitation parameters. Unfortunately, there was not sufficient time to include this. In Figure 3.7, the workflow for the precipitation part is presented.

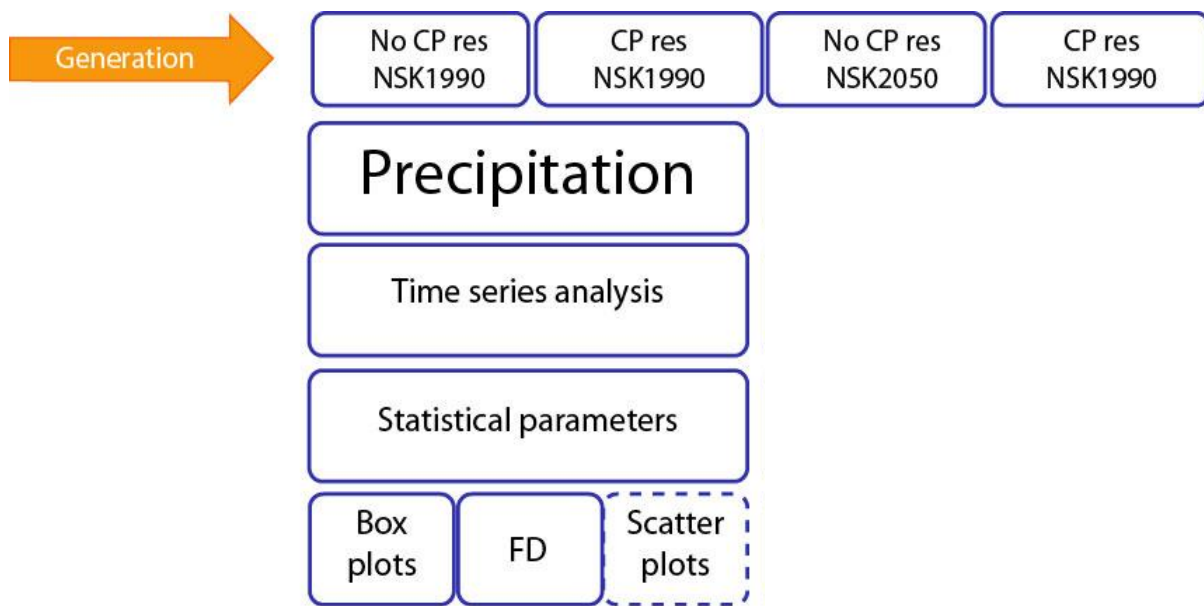


Figure 3.7. Workflow for the precipitation part (Löfvendahl, 2013)

3.3.1 Box-and-whisker plots

One important step when analyzing data and determining the variability for a certain parameter is to initially visualize the data (Massart et.al, 2005). Box-and-whiskers plots are an appropriate way of visualizing data. The box-and-whisker plots are based on robust statistics as this way of presenting data is more resistant to outliers than normally distributed classical statistics. The box-and-whisker plots present the median and the interquartile range (IQR), which are robust ways of describing the central tendency and the dispersion of the data.

The median and the interquartile range are used to construct the box, while the whiskers represent the range of the data (Massart et.al, 2005). The height of the box is equal to the IQR, which represents 50 % of the ranked data. More precisely, the IQR is the range between the lower quartile value, the 25 % percentile, and the upper quartile value, the 75 % percentile. At the location of the median, a horizontal bar is drawn, dividing the IQR into two boxes, representing the lower- and upper quartile.

The whiskers are illustrated as vertical lines, each terminating at the minimum and maximum values with a horizontal line. The whiskers originate from the 25 % percentile for the minimum value and from the 75 % percentile for the maximum value. Figure 3.8, illustrates a box-and-whiskers plot and its components. In the figure, as well as in this study, the mean is also represented in the box-and-whisker plots.

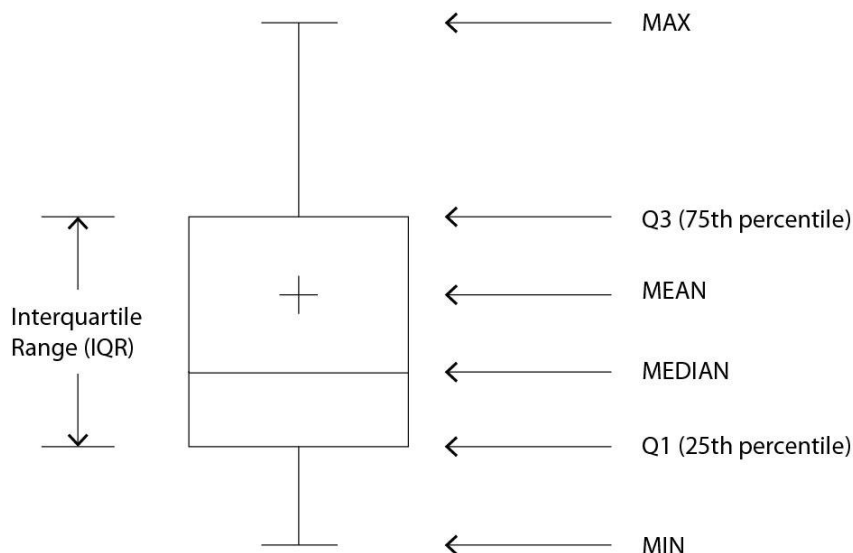


Figure 3.8. The principle of box-and-whiskers plot (SAS/STAT(R) 9.2 User's Guide, Second Edition, 2013). Modified by Jennifer Löfvendahl, 2013

Comparing the dispersion within the IQR between the time-series generated with and without resampling is a robust way of determining the variability. The IQR is determined by more values as the frequency of values are higher around the mean in a distribution, see figure 3.9. The total range is determined by singular, outlying values, which is not a robust way to compare the variability within a population. Thus, the IQR determines the variability in the precipitation parameters within the ten realizations.

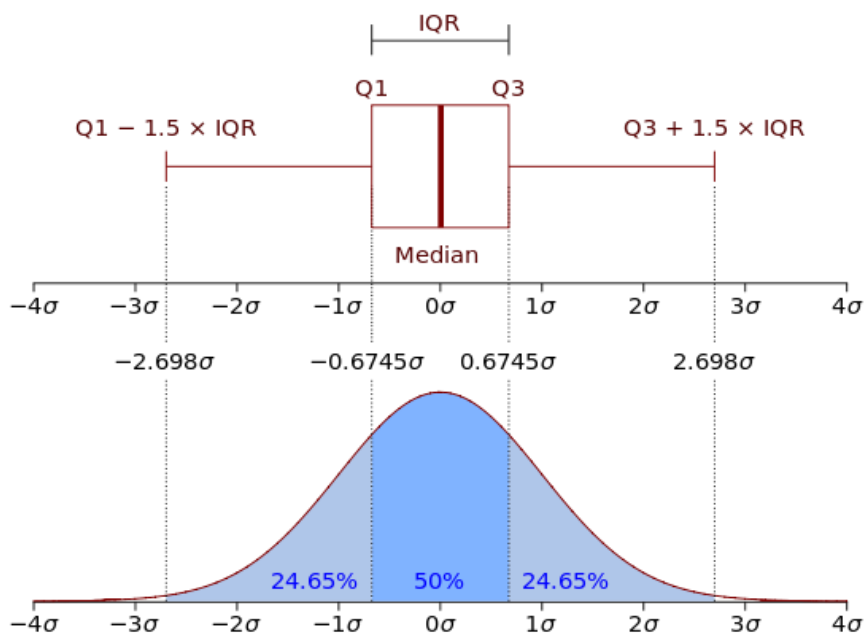


Figure 3.9. The interface between the box-and-whisker plot and a Normal Distribution, (Wikipedia, 2013) modified by Jennifer Löfvendahl, 2013

The following precipitation parameters have been analyzed through box-and-whisker plots in this study:

The yearly precipitation sum

The yearly precipitation sum is often used when describing the precipitation in an area. It is a parameter that differs from the rest because it is accrued over a whole year. The rest of the parameters in this study are in hourly- or daily scale. Due to the long-term scale, the variability in the yearly sum should show a large impact from the resampling of the CP-sequence. As the yearly sum is calculated from the hourly values, the stochastic effect will be averaged out due to the high amount of random numbers, while the CP-Temperature sequence will have a higher impact on the variability in the yearly sum. The variability in the yearly sum is examined for each realization as the long-term average for the ten year time period.

The mean precipitation intensity

The mean of the precipitation intensity is a statistical parameter that is of great importance when determining the variability in generated precipitation data. The mean is the most commonly used measure of the central tendency of data (Massart et.al, 2005). The importance is in its simplicity: it is a well-known statistical parameter that is easy to determine, understand, and compare, and is therefore often used in industry.

However, the simplicity of the mean is also its biggest disadvantage as it is not seen as a robust statistic (Massart et.al, 2005). Extreme values could skew the mean in a manner that is not representative of the entire population. Therefore, it is important that the mean is presented with its confidence interval. The aim of this study is not to determine the mean precipitation intensity from a time-series, but to determine the variability in the generation of the data. Thus, as long as the chosen statistics are calculated in the same way, it is sufficient to compare the mean as a precipitation parameter.

The mean precipitation intensity derived from the precipitation time-series is calculated for the hours and days with precipitation. Consequently, the hours and days with no precipitation (zero values) are not accounted for in the mean precipitation intensity. Calculating the mean precipitation intensity for only wet periods will yield a higher mean intensity. The variability in the mean precipitation intensity is examined for each simulation as the long-term average for the 10 year time period.

Maximum precipitation intensities

As described in Chapter 2.3, a trend towards shorter, more intense events is observable in the scaling properties for the five maximum events in Baden-Württemberg (Beck, 2012). Therefore, the maximum precipitation intensities are important parameters to assess in this study.

Short, intense rain events are often the reason for overflow events in the combined sewer systems. These events occur multiple times a year, and therefore, the maximum precipitation intensities are important parameters when assessing the variability in the precipitation generation. Due to the high-return period and the contribution to overflow events, the 24th maximum precipitation intensity has been included in this study.

The following parameters have been analyzed in order to determine the variability in the maximum precipitation intensities:

1. the maximum precipitation intensity,
2. the median of the 1 - 24th maximum precipitation intensities.

The maximum precipitation intensity is represented by a single value, namely the highest intensity value, for each year in the time-series. For each realization the average value from the 10-year period, the long-term average, is used in the variability analysis. Consequently, only one value represents the maximum intensity of a 10-year period. Thus, this is not a robust statistic as it can vary considerably between the realizations.

The 1 - 24th maximum precipitation median have been calculated for each realization using the mean of the 10 year period for the corresponding maximum intensities. For each realization, the median of the maximum precipitation intensities has been used in the variability analysis. As the analysis for this parameter relies on the median of 24 values, it is considered a more robust way of analyzing data as the extreme values do not affect the result to a significant extent.

The results of the variability in the precipitation parameters will be presented in chapter 4.1.1.

3.3.2 Frequency distribution

A frequency distribution is a convenient way of determining the variability between the synthetic precipitation time-series. By dividing the precipitation time-series into several classes with certain thresholds, the distribution of the hourly- and daily precipitation intensities can be calculated. In this way, the structure of the 10-year precipitation time-series is derived and the variability due to the CP-resampling can be estimated for each class.

In this study, the number of classes was set to 25. Based on the precipitation time-series, appropriate limits for each generation-type were calculated. For the hourly values, the intensities did not differ as much between the four generation types, resulting in the same thresholds with a maximum of 25 mm/h. The minimum threshold was set to 0.1mm/h.

However, for the daily resolution, the intensities differed substantially, resulting in different thresholds for the 25 classes. For the time period NSK1990, the maximum value for the 25th class of the precipitation time-series generated with the same CP-sequence (**No CP res NSK1990**) was 75 mm/d, whereas for the other generation combinations it was 50 mm/d.

Therefore, the classes needed to be combined into a fewer amount with larger threshold-spans in order to be comparable. Instead of 25 classes, the number of classes was decreased to seven.

A frequency distribution can be expressed in either absolute or relative values. The absolute frequency distribution only applies an accumulative structure, adding all values in each class on top of each other. The total number of events in each class and over the 10-year period is calculated in this way. However, when comparing different time-series with each other the total number of events can differ and are not accounted for in the absolute frequency analysis. However, in the relative frequency distribution the total number of events is accounted for as each class is divided by the total number of events for the whole period. In this way, the internal structure, describing the proportion of events occurring in the different classes, of the precipitation during the time period, is presented. Consequently, the relative frequency describes the internal structure of precipitation, whereas the absolute frequency describes the total number of events.

In this study, the variability in the absolute frequency has been analyzed. Thus, the total number of events in each class and not the internal structure of the precipitation time-series is evaluated. The variability between the ten realizations in each class has been determined. The variability, in this analysis represented by the range, is expressed as the difference between the maximum and minimum absolute frequency value between each of the ten realizations in each class, see Figure 3.10. Each bar is represented as one realization and there are 10 realizations in each class.

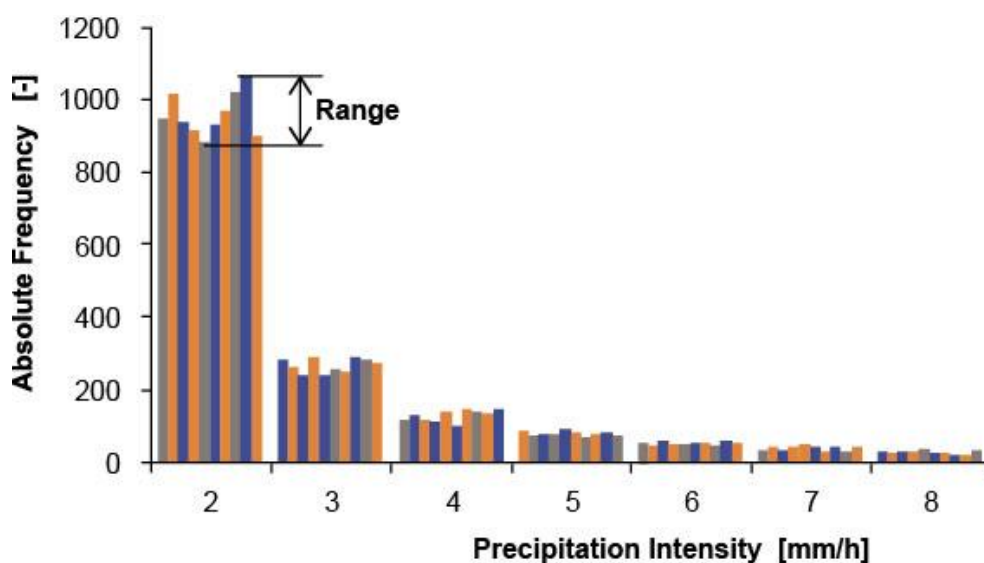


Figure 3.10. Variability in absolute frequency between the realizations (Löfvendahl, 2013)

On hourly scale, the variability due to the resampling of the CP-sequence will not be substantial in the frequency distribution due to the setup of the generator. As mentioned in Chapter 3.1.2, NiedSim-Klima generates time-series in hourly resolution. Thus, a random number for each hour is drawn in the setup of the initial time-series. Regardless of the CP-sequence, the hourly precipitation value is drawn from a beta distribution for intensities smaller than 1 mm/h, and from a Weibull distribution for intensities larger than 1 mm/h. Therefore, the variability in both **No CP res** and **CP res** in the hourly scale will follow the distributions and no significant differences should be visible.

However, on the daily scale, the differences should be more pronounced. As the resampling of the CP-sequence clearly affects the daily precipitation generation, a higher variability due to the resampling is expected.

The results of the variability analysis through absolute frequency distributions are presented in chapter 4.1.2.

3.3.3 Scatter plot

A scatter plot analysis for the precipitation time-series has not been carried out due to time constraints. In a scatter plot analysis, the correlation between two precipitation variables could give an indication of the spread of the variability, which is valuable when assessing the variability due to the stochastic and climatic effect.

3.4 Variability in the CSO overflow characteristics

The variability in overflow characteristic due to the precipitation generation has been determined using long-term simulations with the drainage model KOSIM. The same precipitation time-series analyzed in the precipitation part has been used as input in the model, see Figure 3.11. The overflow parameters from the simulations have been analyzed using box-and-whisker plots as well as a visual scatter plot analysis. This study aims to determine the sensitivity of the urban drainage system due to different precipitation generation realizations, and therefore, the long-term averages have been analyzed. Similar to the precipitation part, a frequency distribution that describes the variability between the different realizations within classes of different overflow volumes was part of the objective as well. However, due to time constraints, the frequency distribution could not be included.

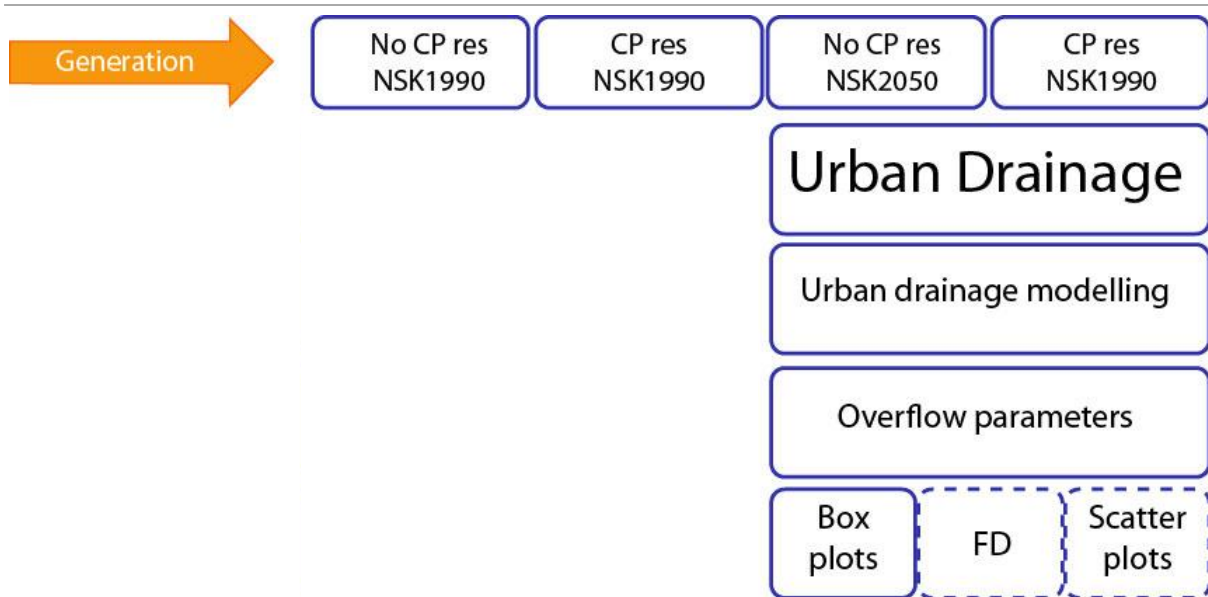


Figure 3.11. Workflow of the urban drainage part (Löfvendahl, 2013)

In the analysis of the variability in the overflow parameters, box-and-whisker plots as well as a visual scatter plots analysis have been used to interpret the variability. The following chapters will describe the methods used and the investigated parameters in more detail.

3.4.1 Box-and-whisker plots

The theory behind box-and-whisker plots is thoroughly described in Chapter 3.3.1. Similar to the precipitation part, the IQR determines the variability in each overflow parameter. The variability within the following overflow parameters has been investigated in this study:

Yearly mixed inflow

The yearly mixed inflow describes the yearly sum of the total combined flow entering the CSOs. The yearly mixed inflow is measured in cubic meters per year. The daily wastewater flow in the CSO is constant. Thus, the magnitude of the yearly mixed inflow is mainly controlled by rain events and the losses occurring before the stormwater enters the pipe-network.

The yearly mixed inflow is a parameter that is directly affected by the precipitation patterns. The parameters contributing to the inflow volume are rain intensity, duration of the rain event, and runoff surfaces. As the catchments are the same in each simulation, only the precipitation parameters can differ and affect the inflow volume.

Yearly overflow

The yearly overflow describes the yearly sum of the total overflow volume in the CSOs and is measured in cubic meters per year. The amount of overflow is dependent on the inflow and the system response. The volume and the duration of a rain event are the essential parameters contributing to an overflow event. If the tank volumes are enough to retain the flow, then a potential overflow event could be prevented.

The yearly overflow is the most essential parameter to investigate as it describes the amount of combined flow released into the watercourse each year. The difference in precipitation generations and how they affect the yearly overflow is important to investigate as it is a commonly used parameter in the industry.

Overflow duration

The overflow duration is a parameter describing the length of an overflow event and is measured in hours per year. The overflow duration is mainly affected not only by the intensity and duration of the rain event, but also by the system response and the tank volume of the CSOs with a storage tank.

Number of days per year with overflow

There are numerous theories of describing a rain- and overflow event. The main difficulty is determining if two events are separated or originate from the same event. One way to present the overflow properties as events, but at the same time avoiding the definition of an event, is to describe the number of days with overflow. A day with overflow is defined as a calendar day when an overflow event occurs, regardless of the volume and the duration of the event.

The results of the variability in the overflow parameters through box-and-whisker plots will be presented in chapter 4.2.1

3.4.2 Frequency distribution

Due to time constraints, a variability analysis through a frequency distribution could not be conducted. In this study, the long-term average parameters are investigated. However, a frequency distribution should be event-specific. The classes should be divided within certain thresholds, and the overflow volume released in each event should be calculated depending on the classes. The same procedure would be possible even for the duration of the event.

Determining the variability through frequency distributions is a preferred method as the variability in the internal structure can be determined. For further studies a variability analysis through a frequency distribution for the overflow parameters is suggested.

3.4.3 Scatter plot

A regression analysis is a statistical tool used to describe the relationship between two observed parameters (Büchse et.al., 2007). A regression analysis is a mathematical estimation method, computed to predict the expected mean of a response variable for a chosen value of a predictor variable. Within a scatter plot, a regression analysis can be presented graphically at locations where the relationship between parameters can be analyzed. In this study, only a visual interpretation of the regression analysis through a scatter plot has been performed in order to analyze the spread of the correlated overflow parameters.

In the scatter plot, the correlation between the yearly overflow volume and the overflow duration has been investigated.

The results of the variability in the visual scatter plot analysis will be presented in chapter 4.2.2.

4 Results

In this chapter, the results from the variability analyses is presented. The main objective is to determine the variability due to the climatic- and stochastic effect.

As there are no previous studies made on this specific topic, the analysis of the results is based on qualified assumptions regarding the outcome of the results. The assumptions are based on theoretical knowledge of the behavior of precipitation, the generation of time-series, and statistical analysis.

4.1 Variability in the synthetic precipitation data

The resampling of the CP-sequence adds an extra source of variability, namely the climatic effect, in the generation of the precipitation time-series. Thus, the IQR for the precipitation time-series generated with a new CP-sequence, **CP res**, should be larger than for the time-series generated with the same CP-sequence, **No CP res**.

How the variability will be affected by climate change is not yet known. As mentioned in Chapter 3.1.3, the different CP-Temperature classes and their respective precipitation response are assumed to be the same even in the future. Only the sequence in which the CPs occur will be different in the future. Therefore, the aim of this thesis is not to determine the variability of climate change independently, but to examine how, as an input for the NiedSim-Klima generator, the variability is altered through climate change.

In the following chapters, the results will be presented and analyzed according to the statements above.

4.1.1 Box-and-whisker plots

The following results were obtained from the variability analysis through box-and-whisker plots for the precipitation parameters:

Yearly precipitation sum

When comparing the interquartile ranges between the **No CP res** and the **CP res** for both the past and the future, it becomes clear that the resampling of the CP-sequence induces a higher variability in the yearly precipitation sum, see Figure 4.1. The results are consistent with theory, and the variability due to the climatic- and stochastic effect can be determined.

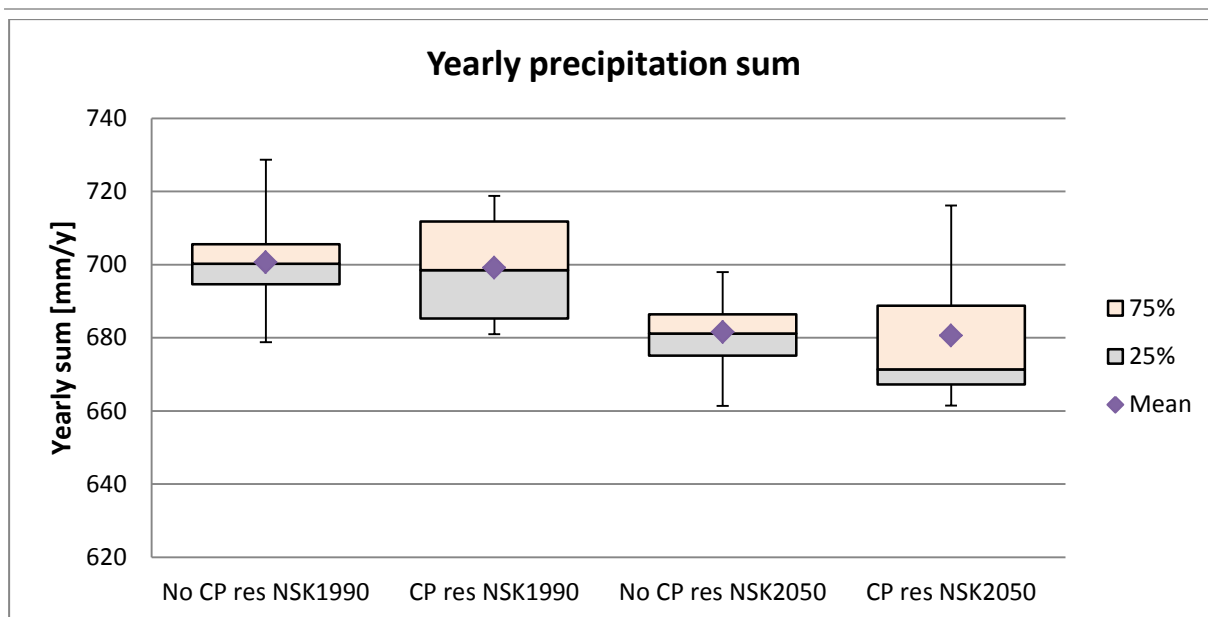


Figure 4.1. Variability in the yearly precipitation sum

However, the **No CP res** for the time period NSK1990 seems to include more wet years as the whiskers, which represents the extreme values, show a higher range with higher intensities than the **CP res** for the same time period. The range between 680 and 730 mm/y is not an extreme range in the yearly precipitation sum when comparing with real precipitation. As mentioned in Chapter 2.2, the variability in yearly precipitation for Baden-Württemberg is between 550 to 850 mm/y. However, the results are realistic as it is the variability in the long-term averages that are investigated. The fact that only a 10 year period and only one station is used also affects the range. As the outlying values are based on fewer statistics, the interquartile range is the main parameter describing the variability. However, the fact that the **No CP res NSK1990** seems to include more wet years than the **CP res NSK1990** is notable as it is also visible in other parameters in this study.

Comparing the time-series generated with a new CP-sequence, **CP res**, for the past and the future, climate change seems to decrease the mean- and median values. The lowering of the the mean and the median is an indication towards smaller precipitation sums in the future.

Mean precipitation intensity

The resampling of the CP-sequence induces a higher variability in the hourly mean precipitation intensity for both the past and the future, see Figure 4.2. From this, the variability due to the stochastic- and climatic effect can be estimated. The resampling of the CP-sequence seems to decrease the mean and median and make the distributions more right-skewed for both the past and the future. A lowering of the mean and the median is an indication of lower

hourly precipitation intensities due to the resampling. A more right-skewed distribution is an indication that more events will be in the left part of the distribution, meaning that more events will have a lower intensity.

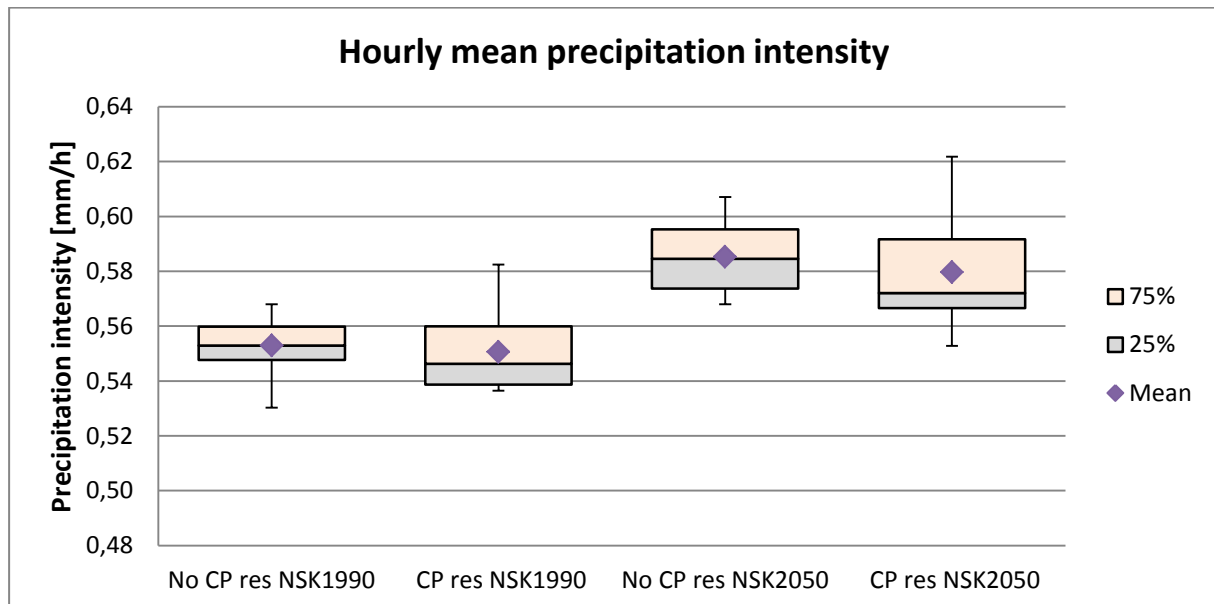


Figure 4.2. Variability in the hourly mean precipitation intensity

Climate change seems to increase the mean and the median for the future. The increase indicates higher hourly mean precipitation intensities in the future. Thus, higher intensities are predicted. These results are consistent with the trends for Central Europe and Baden-Württemberg, as described in Chapter 2.3.

On the daily time scale, an increase in the variability due to the resampling of the CP-sequence is present for both the past and the future, see Figure 4.3. Thus, the variability due to the stochastic- and climatic effect can be determined. Similar to the hourly scale, a trend towards lower precipitation intensities and more right-skewed distributions is present.

However, the trend is not as pronounced as for the hourly scale, and even higher intensities can be expected on the daily scale. The mean and median for NSK1990 is even increasing for the **CP res** when compared to the **No CP res**. This is due to the fact that, when the daily values are aggregated, there is an additional source of variability in the generation. As described in the theory chapter, NiedSim-Klima generates time-series in hourly resolution. Therefore, in the Simulated Annealing optimization, the hourly values will not change the frequency distribution.

When aggregating the hourly values into a daily precipitation value, the frequency distribution will change depending on the sequence of hourly precipitation intensities. Thus, a higher variability is present in the generation of daily precipitation time-series.

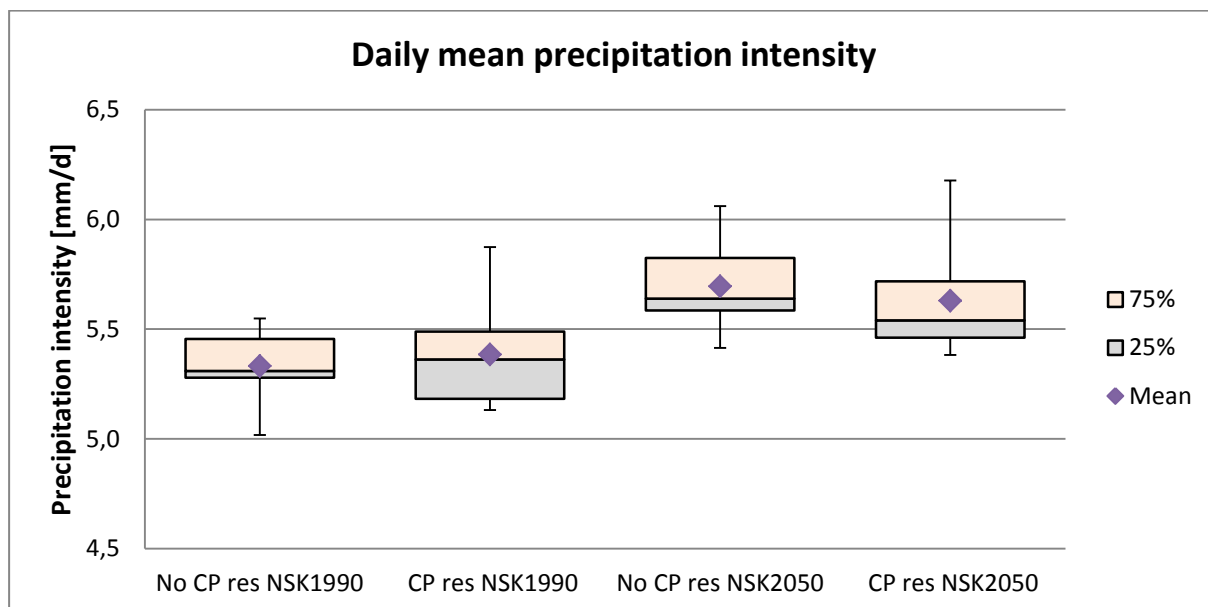


Figure 4.3. Variability in the daily mean precipitation intensity

Climate change seems to increase the mean and the median which indicates an increase in the daily precipitation intensity in the future. This is consistent with the trends described in Chapter 2.3.

Maximum precipitation intensity

The resampling of the CP-sequence induces a higher variability in the hourly maximum precipitation intensity, see Figure 4.4. Thus, the variability due to the stochastic- and climatic effect can be evaluated.

However, the changes are not as profound as for other precipitation parameters. The low variability due to the climatic effect is a result that is consistent with theory due to the generation of the time-series. The variability in the hourly maximum precipitation intensity should follow the Weibull distribution and should be negligably affected by the climatic effect. Only one value is investigated for each year, realization, or generation type, and this is a value that is above 1 mm/h and therefore drawn from the Weibull distribution. Thus, the CP-sequence only has a small influence on the hourly maximum precipitation intensity.

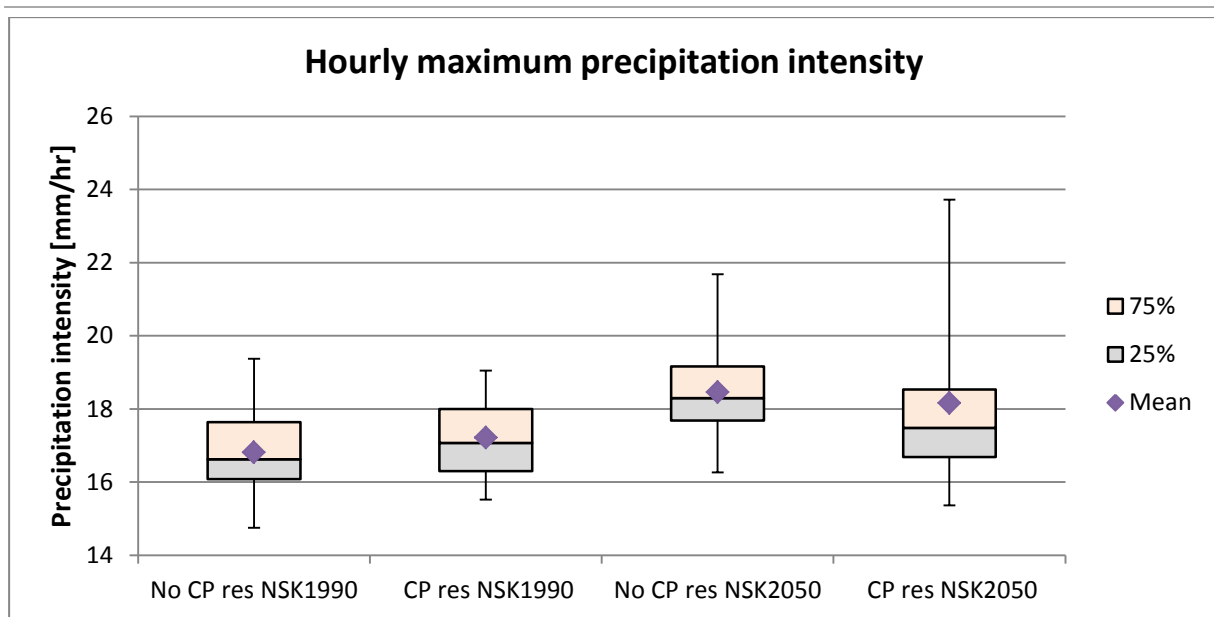


Figure 4.4. Variability in the maximum precipitation intensity

The hourly maximum precipitation seems to increase in the future due to the increase of the mean and median. This is a result that is consistent with theory. The interpolated scaling properties for Baden-Württemberg also show a trend towards higher intensities for the maximum precipitation in the future.

On the daily time scale, an increase in variability due to the resampling of the CP-sequence is present for the past, but not for the future, see Figure 4.5. The maximum precipitation intensity is based on only one value in a 10-year period. Thus, the variability is not as robust as for other investigated parameters which are based on more values.

Climate change seems to lower the median and mean for the future scenario. The lowering of the mean and median is an indication of lower daily maximum intensities in the future. This outcome is not consistent with theory as the daily extreme intensities are expected to increase according to the theories described in chapter 2.3. As mentioned in the methodology, it is not a robust way to analyze only one value, and yet, the variability for the future precipitation intensities should be generally higher. The reason for this outcome is unknown, future investigations with the IWS department is necessary.

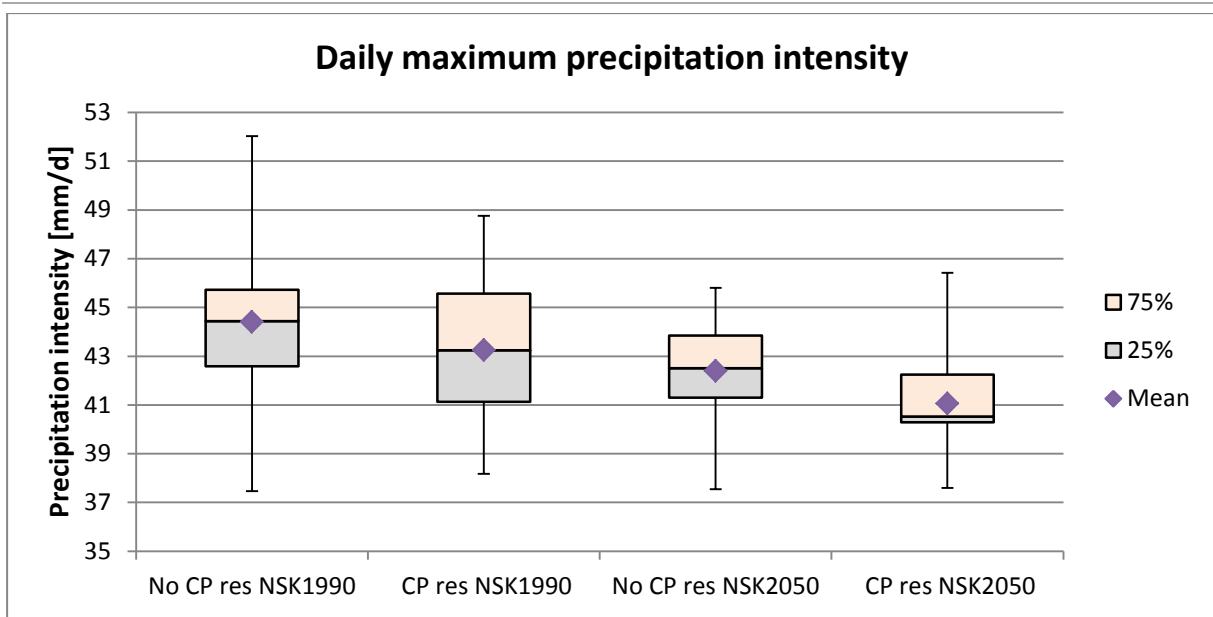


Figure 4.5. Variability in the daily maximum precipitation intensity

Median of the 1 - 24th maximum precipitation intensities

The resampling of the CP-sequence induces a higher variability in the median of the 1 - 24th hourly maximum precipitation intensities, see Figure 4.6. Thus, the variability due to the stochastic- and climatic effect can be evaluated. The mean and the median are decreasing due to the resampling of the CP-sequence. The decrease indicates lower intensities due to the CP-resampling.

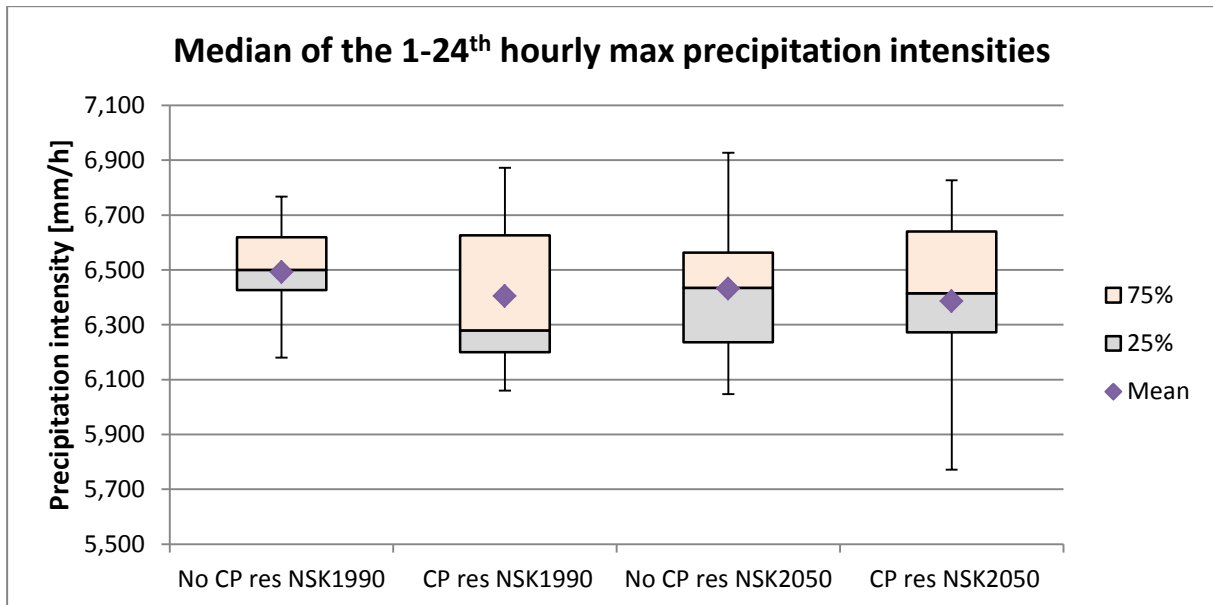


Figure 4.6. Variability in the median of the 1 - 24th maximum hourly precipitation intensities

The same increasing trend in future hourly maximum intensities should be visible even in the median of the 1 - 24th hourly maximum. However, the mean and the median are decreasing for **No CP res NSK2050** compared to **No CP res NSK1990**, which indicates a decrease in maximum intensity in the future.

When comparing the time-series generated with a new CP-sequence, **CP res**, for the past and the future, the median increases for the future while the mean stays the same, see Figure 4.6. Thus, the distribution becomes more left-skewed in the future which is an indication towards higher intensities. This result is consistent with theory. However, there are uncertainties in the manner NiedSim-Klima generates extreme values. Therefore, this needs to be investigated further with the IWS.

Even on the daily time scale, an increase in the variability due to the resampling of the CP-sequence is present, see Figure 4.7. Thus, the variability due to the stochastic- and climatic effect can be evaluated. The mean and median increases due to the resampling which indicates higher intensities due to the resampling of the CP-sequence.

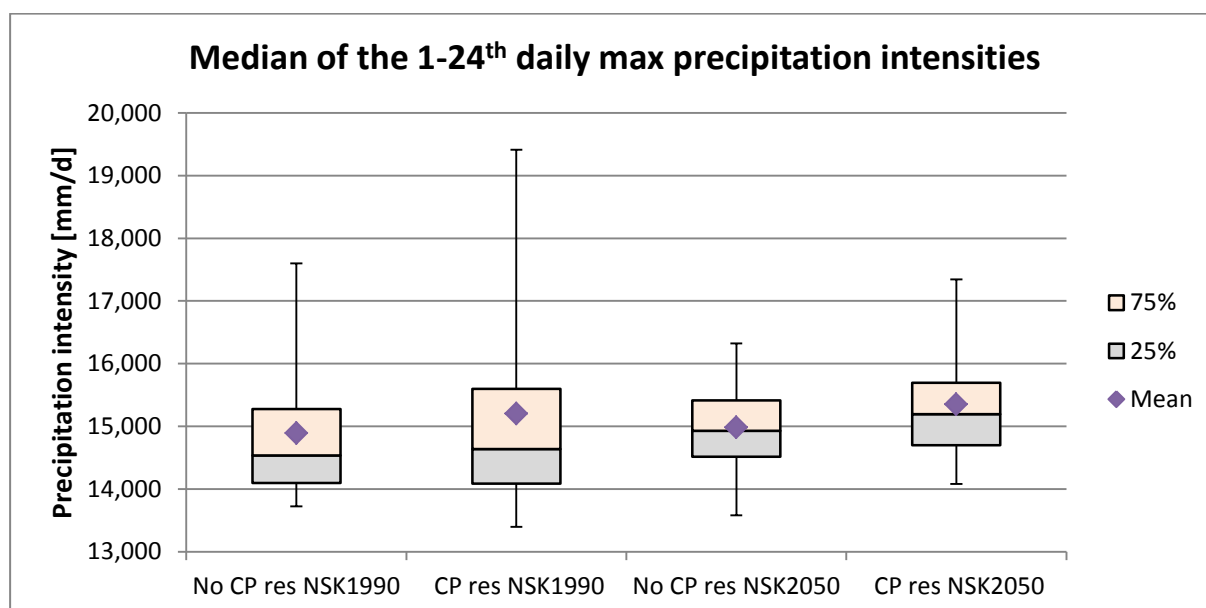


Figure 4.7. Variability in the median of the 1 - 24th daily maximum precipitation intensities

The median seem to increase due to climate change, which indicates higher daily intensities. The mean, however, seems to stay the same. That the median value increases and the mean stays the same indicates that the distributions for NSK2050 becomes more left-skewed compared to the NSK1990 distributions and thus an increase in the intensity due to climate change.

As an example for future studies, the magnitude of the total variability which is due to the climatic- and stochastic effect has been calculated for each of the investigated parameters, see Table 4.1. The total variability is represented by the IQR for the time-series generated with a new CP-sequence for the past, **CP res NSK1990**.

	Yearly sum	Hourly mean	Daily mean	Hourly max	Daily max	Hourly 1-24th median max	Daily 1-24th median max
Climatic effect	59	43	42	8	29	55	22
Stochastic effect	41	57	58	92	71	45	78

Table 4.1. Part of the total variability due to the climatic- and stochastic effect.

The yearly sum varies between 670 to 729 mm/y due to the stochastic effect. Including the climatic effect, the yearly sum varies between 659 and 738 mm/y. Thus, the climatic effect represents almost 60 % of the total variability in the yearly sum, as seen in Table 4.1. As mentioned in Chapter 3.3.1, the yearly sum is a parameter that is highly affected by the resampling of the CP-sequence.

The hourly mean precipitation intensity varies between 0.55 and 0.56 mm/h due to the stochastic effect. Including the climatic effect, the hourly mean precipitation varies between 0.53 and 0.56 mm/h. While the climatic effect is significant, the stochastic effect proves to have a higher influence of roughly 57 %. The daily mean precipitation intensity shows the same results: a higher influence from the stochastic effect of about 58 %, but also a significant influence from the climatic effect. The daily mean intensity varies between 5.3 and 5.5 mm/d due to the stochastic effect and, when including the climatic effect, it varies between 5.2 and 5.5 mm/d.

The hourly maximum varies between 16.1 and 17.6 mm/h due to the stochastic effect. Including the climatic effect, the hourly maximum varies between 16.3 and 18 mm/h. Thus, only 8 % of the total variability is due to the climatic effect. The remaining 92 % is due to the stochastic effect. As mentioned in the results chapter for the hourly maximum precipitation intensity, this has to do with the generation of intense precipitation intensities.

The daily maximum varies between 42.6 and 45.7 mm/d due to the stochastic effect. Including the climatic effect, the daily maximum varies between 41.1 and 45.6 mm/d. Thus, the daily maximum is also mostly affected by the stochastic effect to about 71 %, but the climatic effect has a higher influence on the daily than for the hourly maximum, which is consistent with expectations.

The median of the 1 - 24th hourly maximum varies between 6.4 and 6.6 mm/h due to the stochastic effect. Including the climatic effect, the median of the 1 - 24th hourly maximum varies between 6.2 and 6.6 mm/h. This results in a high influence from both the stochastic and climatic effect, about 55 % and 45 % respectively.

The median of the 1 - 24th daily maximum shows a different result. The median varies between 14 mm/d and 15.2 mm/d due to the stochastic effect. Including the climatic effect, the median of the 1 - 24th daily maximum varies between 14 mm/d and 15,6 mm/d. This results in a major influence from the stochastic effect of about 78 % and a minor influence from the climatic effect.

4.1.2 Frequency distribution

In Figure 4.8 and 4.9 below, the absolute frequency in the daily precipitation intensities for every realization in each selected class is presented. Figure 4.8 represents the precipitation time-series generated with the same CP-sequence for the past on a daily scale, **No CP res NSK1990**. Diagram 4.9 represents the time-series generated with a new CP-sequence for the past on a daily scale, **CP res NSK1990**. Considering the difference between the highest and lowest values of each column, it becomes clear that there is heterogeneity in the absolute frequency between the different realizations for time-series generated with and without resampling.

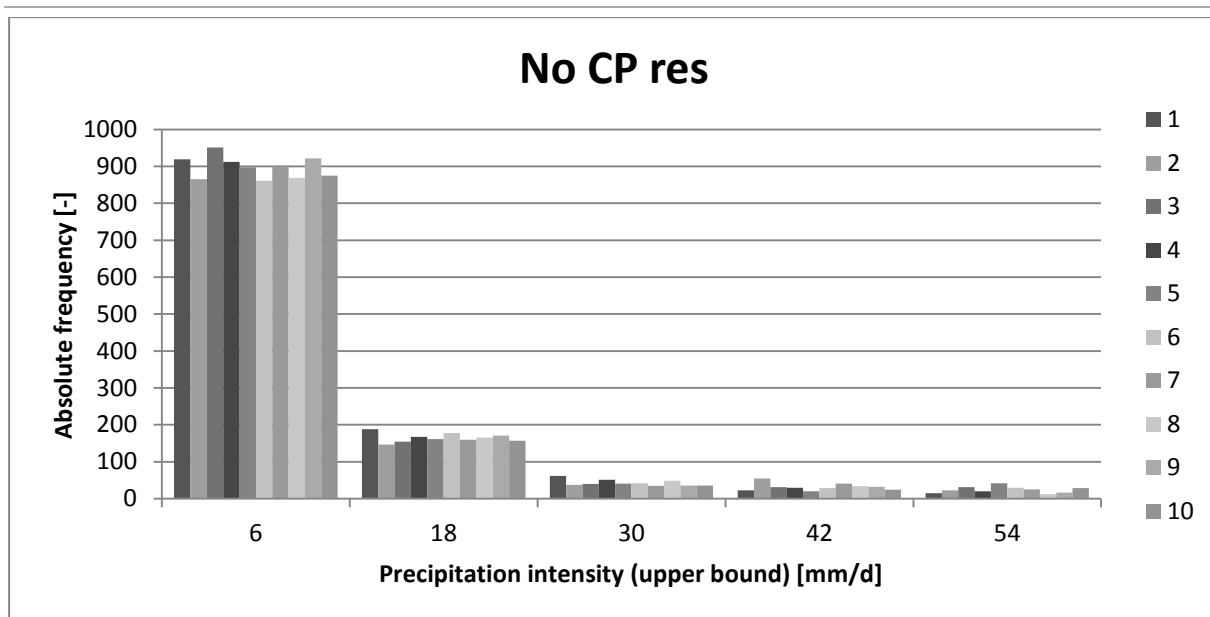


Figure 4.8. The absolute frequency for each of the 10 time-series generated with no CP-resampling

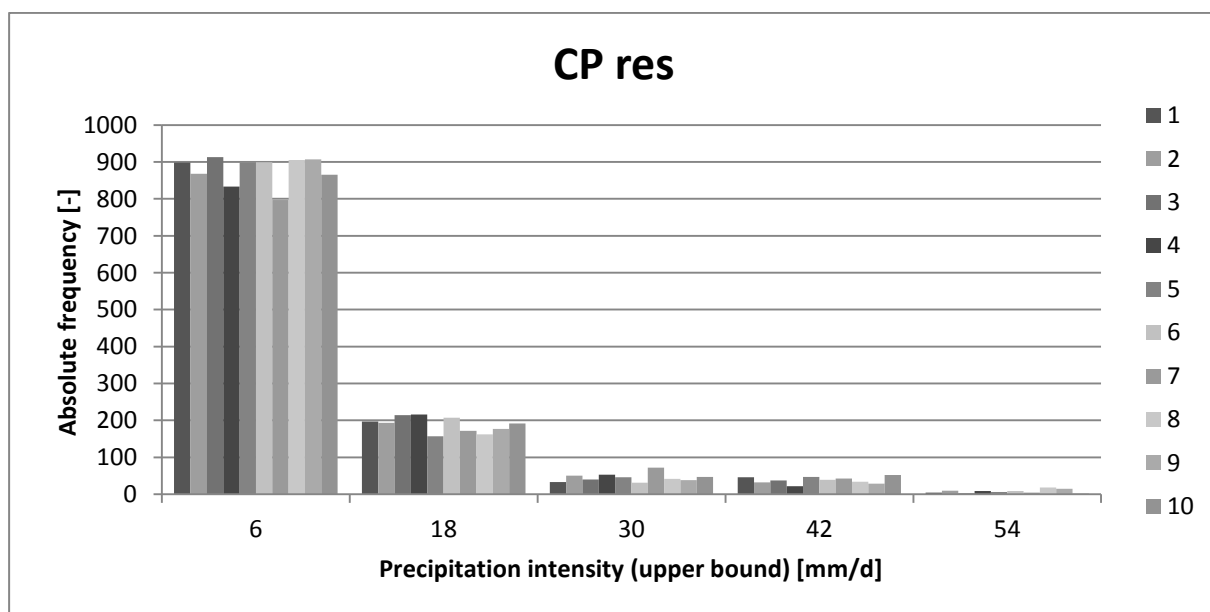


Figure 4.9. The absolute frequency for each of the 10 time-series generated with CP-resampling

By a rough estimation comparing Figure 4.8 and 4.9, one could expect a higher variability in the generation with a new CP-sequence, **CP res**, which would be consistent with theory. However, in the classes with the higher intensities, the generation with the same circulation pattern sequence, **No CP res**, shows higher frequencies and also a higher variability. When estimating the variability further and by comparing the range in each class, the rough estimation proved to be true.

Additionally, for the **No CP res**, the two last classes with higher intensities (total upper boundary = 78 mm/d) had to be removed from this analysis, as the **CP res** did not include intensities in that range.

In the Figure 4.10 below, the difference in range between the **CP res** and the **No CP res** in each class is presented. Here, it becomes clear that the CP-resampling induces a higher variability for the classes with lower intensities. However, for the classes with a higher intensity, the variability decreases due to the resampling of the CP-sequence. The events in the higher classes are extreme and occur very rarely. This outcome is not consistent with the expectations; the variability due to the climatic effect should be visible in each class. The reason for this outcome is unknown and further investigations in cooperation with the developers of the NiedSim-Klima generator at IWS are necessary.

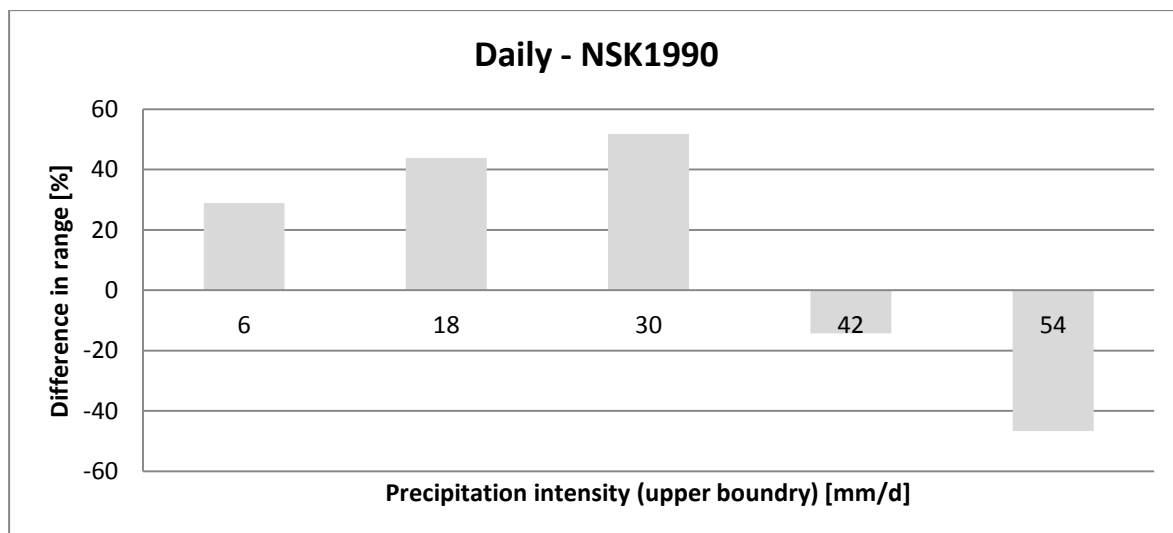


Figure 4.10. Difference in range between the CP res and No CP res for the time period NSK1990

The same method is used on the daily scale for the future scenario, NSK2050. Here, a different outcome is present and the climatic effect only seems to induce a higher variability in the middle intensities. For the lower and highest intensities, the climatic effect seems to decrease the variability. Another result worth noticing is that the total variability seems to be less for the future scenario than for the past. The expectations were that it should have been the opposite: a higher variability in the future due to the climatic effect. As mentioned above, the climatic effect should increase the variability in each class. Why the results did not fulfill expectations are unknown, and further studies in cooperation with IWS must be carried out.

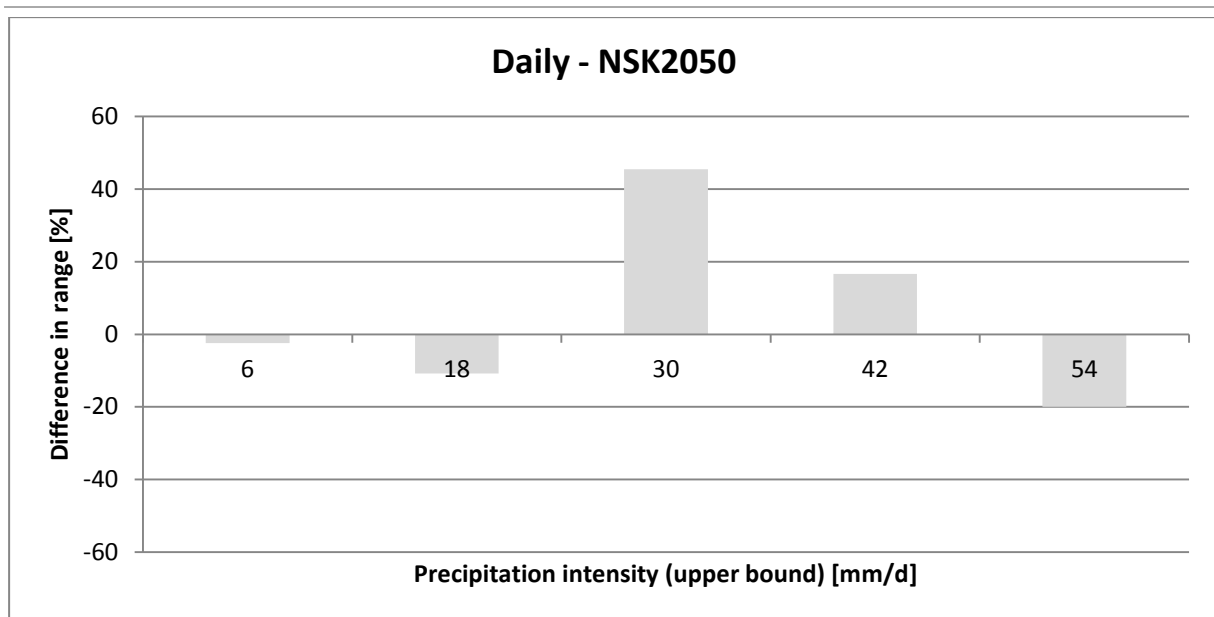


Figure 4.11. Difference in range between the **CP res** and **No CP res** for the time period NSK2050

The variability in the frequency distributions on the hourly scale has also been investigated. As mentioned in the method chapter, 25 classes were used in the setup of the frequency distributions on the hourly scale. However, only 10 classes are presented for visibility and analysis reasons. About 90 % of the total values are in classes 1 and 2, with the remaining 10 % divided among the other 23 classes with a decreasing trend. There are not enough values in the higher classes for a robust analysis, and therefore 10 classes have been chosen as a threshold, which represents 99.5 % of the total values in the distribution.

As mentioned in Chapter 3.3.2, the resampling of the CP-sequence should not induce a high variability in the frequency distributions on the hourly scale. Regardless of the CP-sequence, the hourly precipitation value is drawn from a Beta distribution for intensities lower than 1 mm/h, and from a Weibull distribution for intensities higher than 1 mm/h. Therefore, the variability in both **No CP res** and **CP res** will follow the distributions and no significant differences should be visible. However, differences are found for both the past- and future scenarios, see Figure 4.12 and 4.13. This outcome was not expected and future investigations with the IWS are necessary.

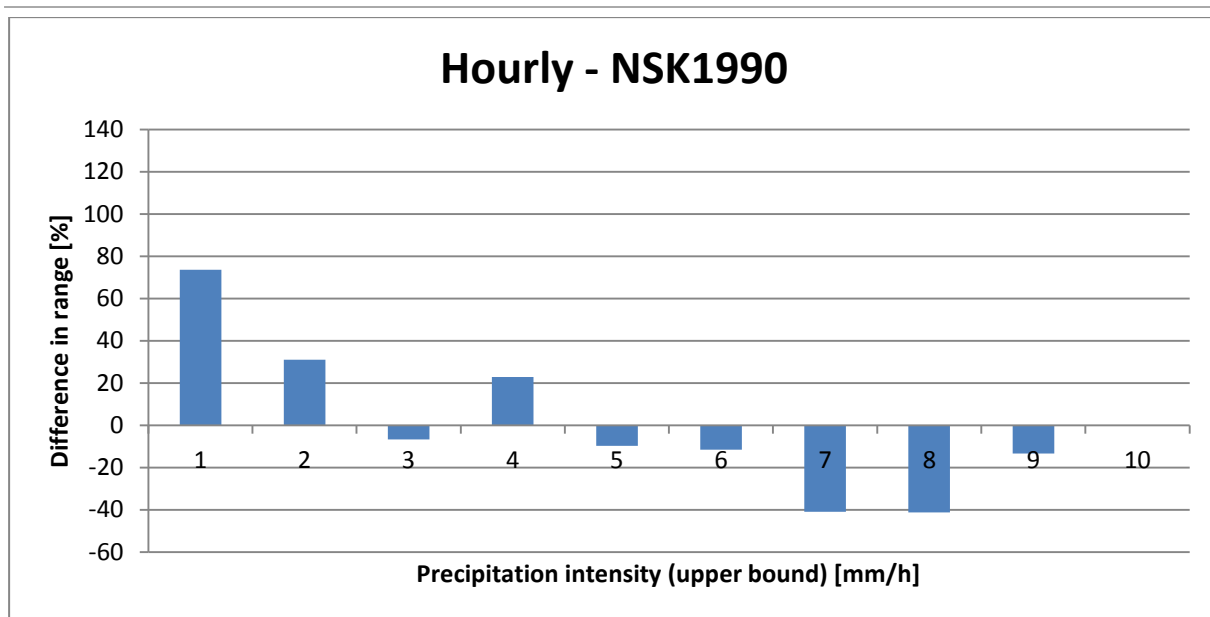


Figure 4.12. Difference in range between the CP res and No CP res on hourly scale for the time period NSK1990

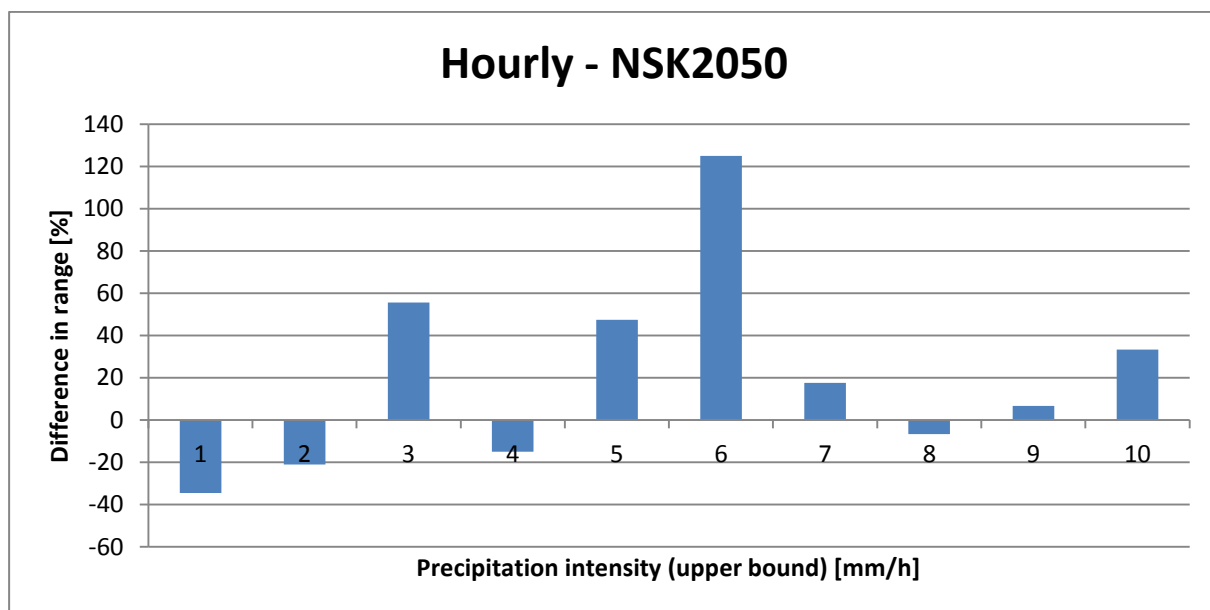


Figure 4.13. Difference in range between the CP res and No CP res on hourly scale for the time period NSK2050

An interesting discovery for both the daily and hourly frequency distributions is that the resampling seems to have an effect on the lower intensities for the past but not for the future. In the future scenario, the variability seems to decrease due to the resampling of the CP-sequence. As the lower intensities represents about 90% of the total values, the effect of the resampling should be visible in these intensities even in the future.

4.1.3 Summary

The results from the precipitation part show an increase in variability due to the resampling of the CP-sequence through the box-and-whisker plot analysis. Thus, the influence of the climatic- and stochastic effect in the total variability can be determined.

In the analysis of the effect of climate change on the precipitation parameters, almost all the parameters were consistent with the trends. However, the maximum intensities are predicted to increase in both the hourly- and daily scale, which was not the case for all investigated maximum parameters. Further investigations with the IWS department are necessary.

The frequency distributions on both the hourly- and daily scale did not present the expected results. For the daily scale, including the climatic effect did not increase the variability in all classes as expected. On the hourly scale, the differences were pronounced even though the distribution of the absolute values on the hourly scale should not differ. Similarly for the box-and-whisker plot analysis, the maximum intensities in the frequency distribution do not show the expected results. The variability decreases for the highest intensities on the daily scale when including the climatic effect, both for the past and the future. Further investigations in cooperation with IWS are needed.

4.2 Variability in the overflow characteristics

Previous studies have shown that a small difference in the precipitation generation can have a huge impact on the CSO activity. Therefore, to be able to determine the sensitivity of the urban drainage system due to the precipitation generation, the same precipitation time-series used in the variability analysis for the precipitation, have been used in long-term simulations in the urban drainage model KOSIM.

The same principle as for the precipitation generation part is true even for the study of urban drainage: the resampling of the CP-sequence adds an extra source of variability in the generation of the precipitation time-series. Thus, the interquartile range for the long-term simulations with precipitation time-series generated with a new CP-sequence, **CP res**, should be larger than for the simulations with precipitation time-series generated with the same CP-sequence, **No CP res**.

In the following chapters, the results will be presented and analyzed according to the statements above.

4.2.1 Box-and-whisker plots

The following results were obtained from the variability analysis through box-and-whisker plots for the overflow parameters:

Yearly mixed water inflow, VQzu

The resampling of the CP-sequence seems to induce a higher variability in the yearly mixed inflow for both the past and the future, see Figure 4.14. Thus, the variability due to the stochastic- and climatic effects can be determined. The variability seems to have a significant increase due to the climatic effect.

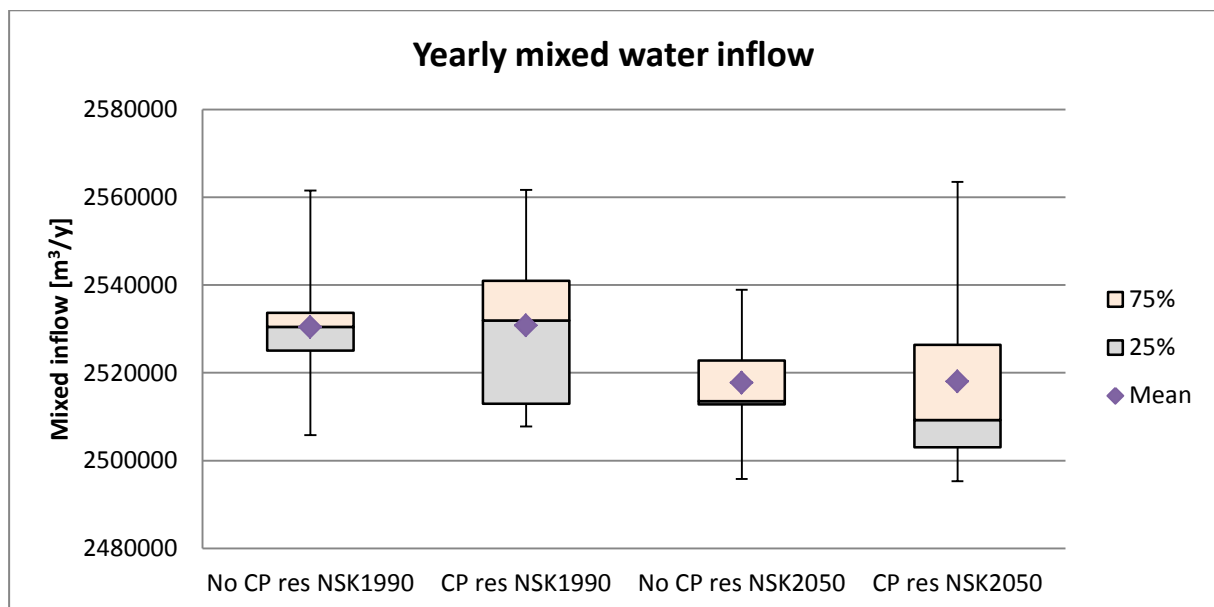


Figure 4.14. Variability in the yearly mixed water inflow

The mean and the median for the future seem to be lower due to climate change, which indicates a decrease in the yearly mixed inflow. This is consistent with the theory and the results presented from the study by Bendel et al (2013), presented in Chapter 2.4. An increasing amount of shorter events are expected in the future, which lead to higher losses of evaporation and infiltration.

Yearly overflow, VQue

The resampling of the CP-sequence seems to induce a higher variability in the yearly overflow for both the past and the future, see Figure 4.15. Thus, the variability due to the stochastic- and climatic effect can be determined.

Generally, the resampling of the CP-sequence causes less overflow for both the past and the future. The **CP res NSK1990** seem more evenly distributed around the mean and median, while **CP res NSK2050** is strongly right-skewed. This indicates less overflow volumes due to the resampling of the CP-sequence.

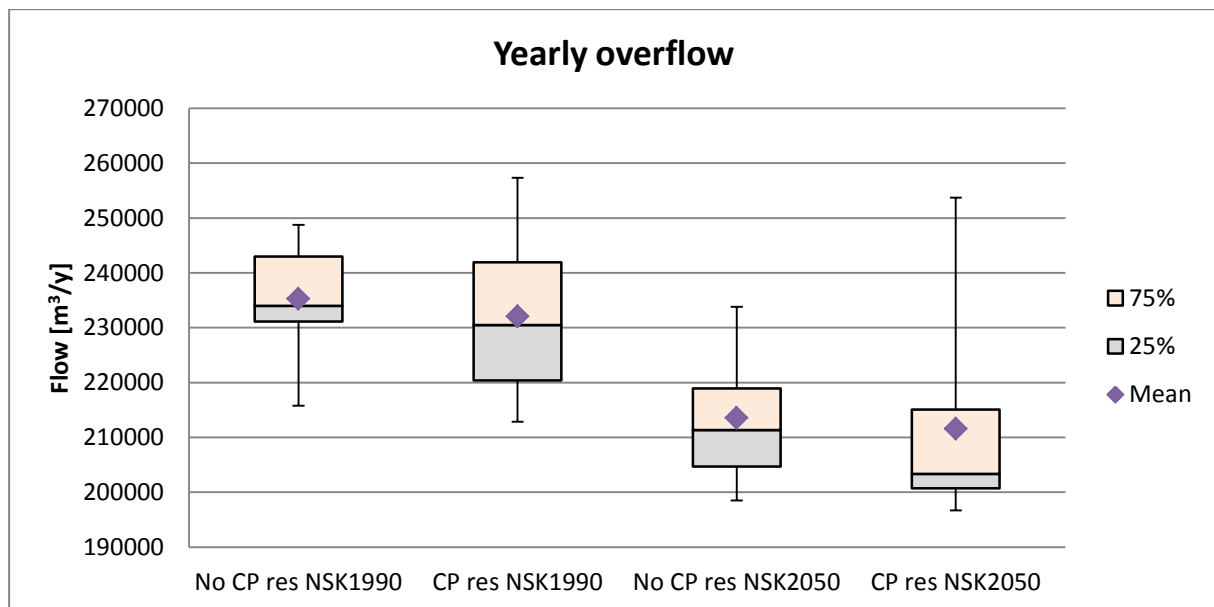


Figure 4.15. Variability in the yearly overflow

Climate change seems to lower the mean and median, and the distributions in the future are significantly right-skewed. This indicates less overflow volumes in the future. The CSOT 10 is placed downstream the CSS network and is responsible of about 70 % of the total overflow volume. According to the study by Bendel et al. (2013), the effects of climate change on yearly overflow volume depend strongly on the type of CSO structure. Bendel et al. (2013) recognized a decrease in the yearly overflow volume for CSO tanks and an increase for regular CSO structures. As the precipitation is expected to be shorter and more intense in the future, these events can be retained in the storage tank to a larger extent, leading to smaller overflow volumes. As the CSOT10 is controlling the major part of the overflow volume, the total response of the system is consistent with the results regarding the CSO tanks.

Yearly overflow duration, T_{ue}

The resampling of the CP-sequence seems to induce a higher variability in the yearly overflow for the past but not for the future, see Figure 4.16. The duration of a rain event is not determined by the sequence of the CP to a significant extent, but rather from the autocorrelation, which is a constraint in the objective function in the Simulated Annealing algorithm. Thus, the variability in the yearly overflow duration is mainly due to the stochastic effect.

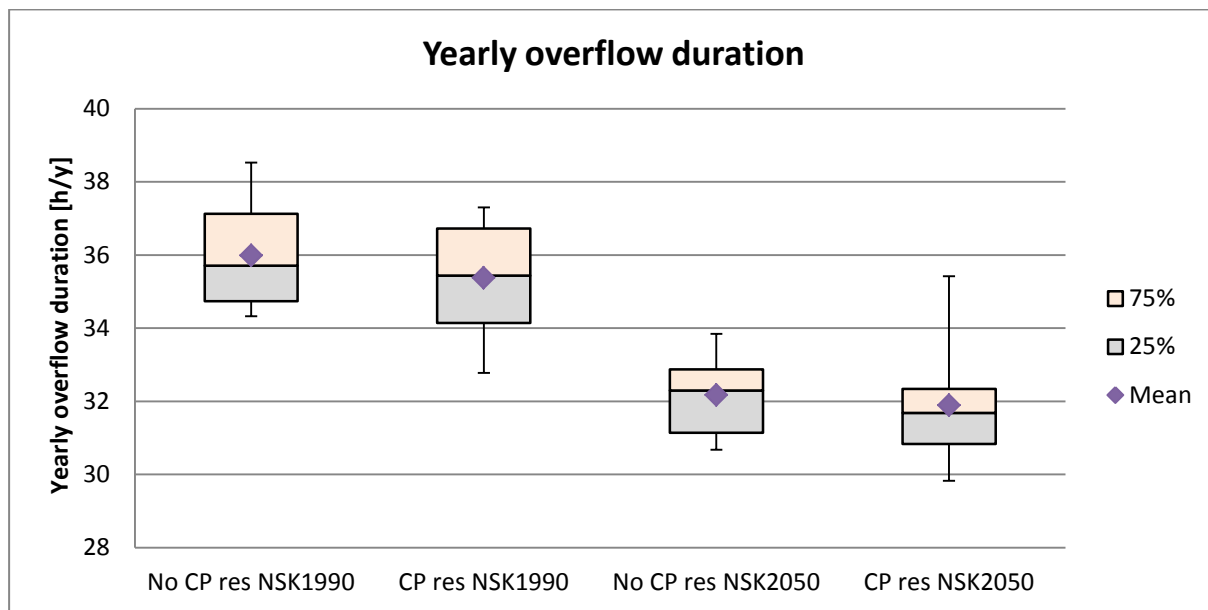


Figure 4.16. Variability in the yearly overflow duration

Climate change seems to lower the mean and median, and the distributions in the future are more right-skewed. This is an indication for lower overflow durations in the future. A pronounced decrease in the yearly overflow duration due to climate change was also found by the previous study by Bendel et al. (2013). The reason for the decrease is due to the shorter, more intense events in the future.

Number of days per year with overflow, $n_{ue,d}$

The resampling of the CP-sequence seems to induce a higher variability in the yearly overflow for both the past and the future, see Figure 4.17. Thus, the variability due to the stochastic and climatic effect can be determined.

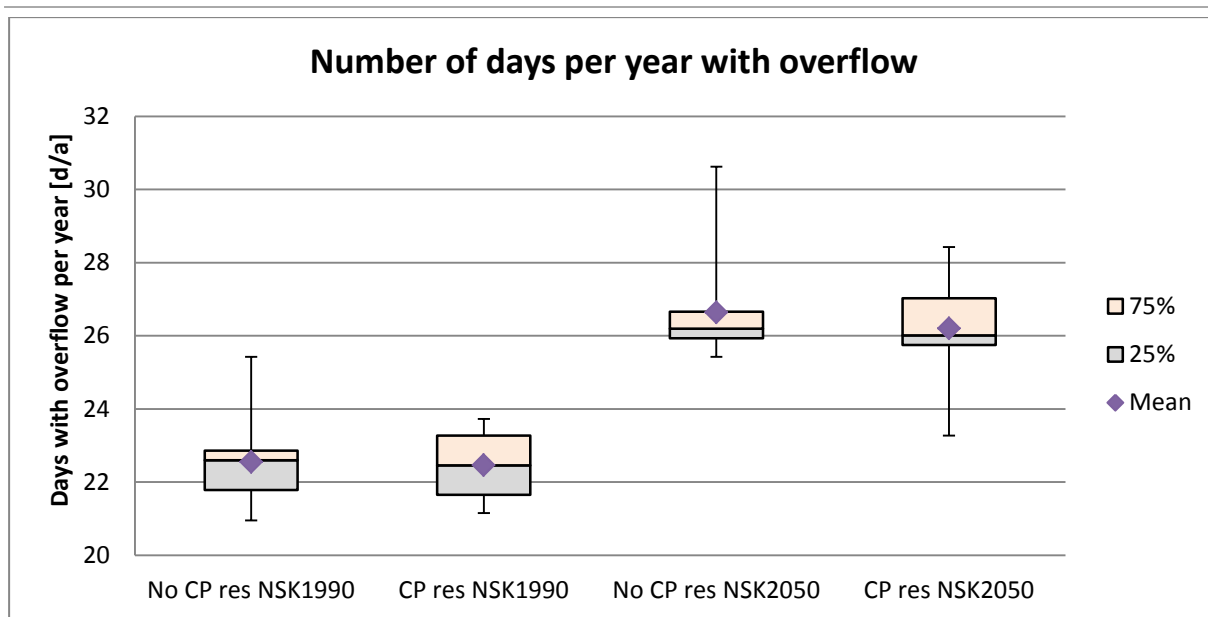


Figure 4.17. Variability in the number of days per year with overflow

Due to climate change, the mean and the median seems to increase. This indicates a trend towards more days with overflow. The same results were obtained in the study by Bendel et al (2013). The events are predicted to become more intense with shorter duration times and higher frequency in the future.

Similar to the precipitation parameters, the section of the total variability which is due to the climatic- and stochastic effect have been calculated for each of the investigated overflow parameters, see Table 4.2. The total variability is represented by the interquartile range for the time-series generated with a new CP-sequence for the past, **CP res NSK1990**.

	VQzu	VQue	T,ue	n,ue,d
Climatic effect	69	45	8	34
Stochastic effect	31	55	92	66

Table 4.2. Part of the total variability due to the climatic- and stochastic effect.

The yearly inflow, V_{Qzu} , varies between 2.52 to 2.53 million m^3/y due to the stochastic effect. Including the climatic effect, the yearly inflow varies between 2.51 to 2.54 million m^3/y . Thus, the yearly inflow is profoundly influenced by the climatic effect. Almost 70 % of the total variability is due to the climatic effect. It seems like a reasonable result as the inflow is mainly affected by the precipitation into the system and not the system response. Similar to the yearly precipitation sum, the variability in the yearly inflow should show a large impact from the resampling of the CP-sequence, which is due to the long time scale.

The overflow volume, V_{Que} , varies between 231 and 242 thousand m^3/y due to the stochastic effect. Including the climatic effect, the overflow volume varies between 220 and 242 thousand m^3/y . Thus, the influence of the climatic- and stochastic effect is both significant, 45 % and 55 % respectively.

The overflow duration, T_{ue} , varies between 34,7 and 37,1 h/y due to the stochastic effect. Including the climatic effect, the overflow duration varies between 34,1 and 36,7 h/y. Thus, the overflow duration is mainly affected by the stochastic effect. Over 90 % of the total variability is due to the stochastic effect. This is a reasonable result as the duration of a rain event is mainly determined by the autocorrelation and only to a small extent affected by the resampling of the CP-sequence.

The overflow frequency, $n_{ue,d}$, varies between 21,8 and 22,8 d/y due to the stochastic effect. Including the climatic effect, the days with overflow vary between 21,7 and 23,3 d/y. Thus, the stochastic effect is more pronounced, representing about 66 % of the total variability.

4.2.2 Scatter plot

Figure 4.18 shows the correlation between the yearly overflow volume and the overflow duration for the past. The red and blue “clouds” are only a visual interpretation of the spread of values. The figure shows that the resampling of the CP-sequence induces a higher variability in the correlation between the yearly overflow and the overflow duration. For a fixed duration time, the precipitation time-series generated with a new CP-sequence generates events with both more- and less-overflow volume. Thus, the climatic effect induces changes in the variability in both directions, which can be visible by the red ellipse surrounding the blue ellipse, representing the cloud of events for each generation type.

Considering a fixed-overflow volume, the variability in the overflow duration is insignificant. The same conclusion is drawn from the box-and-whisker plot analysis: the overflow duration is scarcely affected by the resampling of the CP-sequence.

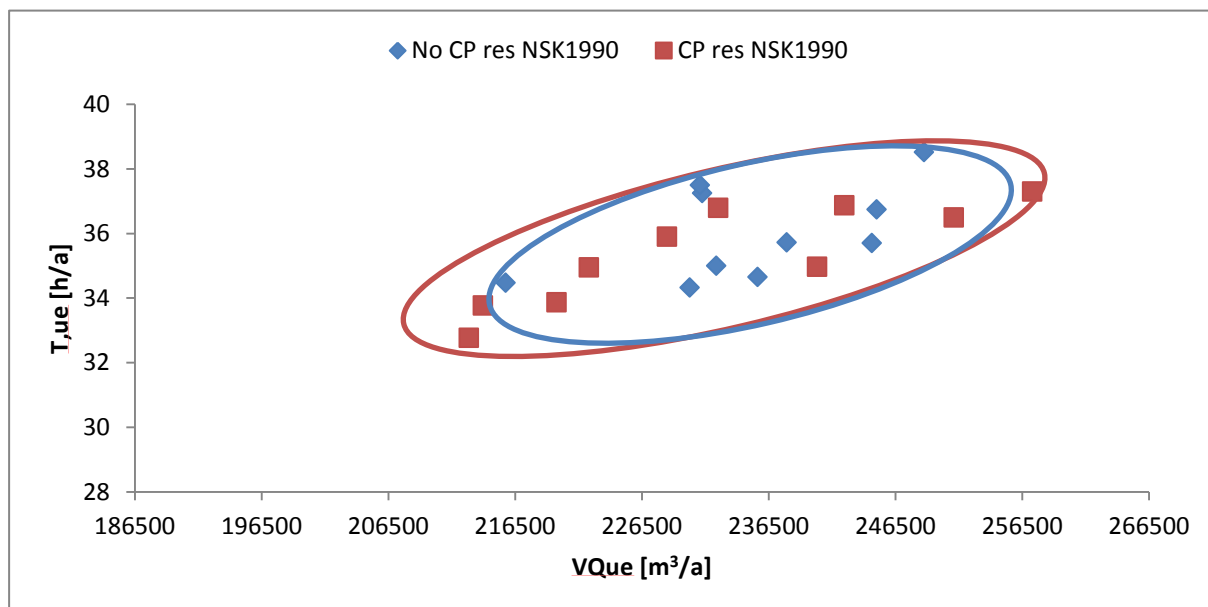


Figure 4.18. Correlation between the yearly overflow volume V_{Que} and the overflow duration $T_{,ue}$ for the past

For the future scenario, the results look similar to the past scenario: an increased variability due to the resampling of the CP-sequence. However, only one value is responsible for the increase in variability. Otherwise, the values seem more condense within the green ellipse, representing the spread of the correlated parameters.

Moreover, a decrease of lower overflow volumes and overflow durations is also visible. This is consistent with the results from the box-and-whisker plot analysis, showing a trend towards lower overflow volumes and duration times.

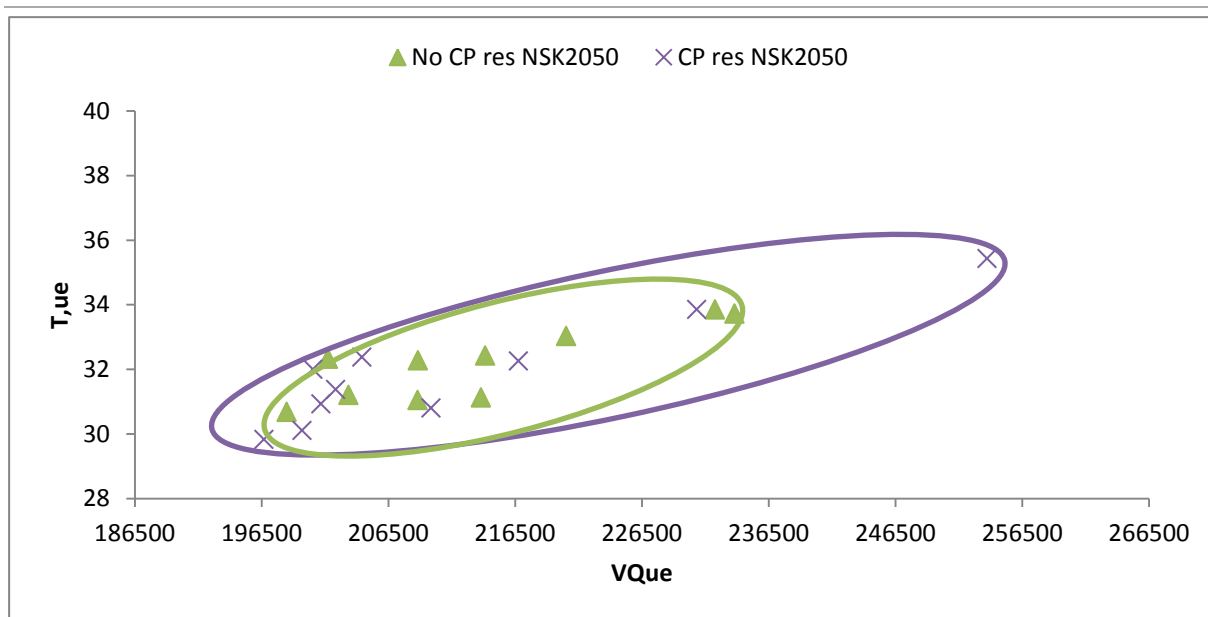


Figure 4.19. Correlation between the yearly overflow volume V_{Que} and the overflow duration $T_{,ue}$ for the future

4.3 Summary

The results for the overflow parameters show an increase in variability due to the resampling of the CP-sequence when comparing the IQR for the **No CP res** and **CP res for NSK1990** in the box-and-whisker plot analysis. Thus, the influence of the climatic- and stochastic effect in the total variability could be determined. The influence in the overflow parameters due to climate change is consistent with the theory and the results from the study by Bendel et al (2013).

For both the past and the future, the scatter plot indicates a higher variability due to the resampling of the CP-sequence when correlated with the yearly overflow and the overflow duration. However, these results are only visually interpreted and a more mathematically correct method would be preferred.

5 Conclusion and outlook

In this chapter, the results and the methods used in this study will be evaluated and concluded. Suggestions on further investigations will also be provided.

5.1 Box-and-whisker plot analysis and number of realizations

In the box-and-whisker plot analysis, the CP-resampling induces a higher variability for almost all the precipitation- and overflow parameters. Thus, the variability due to the climatic- and the stochastic effect can be determined for the precipitation generation and its response in the overflow characteristics. The box-and-whisker plot analysis proved to be an effective method to analyze the variability. As precipitation is highly variable and can be strongly affected by extremes, expressing and comparing variability by the interquartile range proved to be beneficial.

Expressing the variability as the interquartile range removed the focus from the actual influence of the number of realizations in the results. It is still unknown if the number of realizations were enough to express the variability in a robust and correct way. However, the variability increased due to the resampling of the CP-sequence for the majority of the investigated parameters, which is consistent with the theory and the expectations. The range did not increase for all parameters due to the CP-resampling as the extreme values could be determined by only a few values in a population. Even if the number of realizations would increase, there may not be a change in the total range as it is too much affected by the random effect. Thus, the number of realizations proved to be enough for the aim in this study. For future investigations, the number of realizations has to be balanced to serve its purpose.

5.2 Frequency distribution

For the precipitation, the variability in the absolute frequency distribution on a daily scale for the past was not consistent with expectations. An increase due to the CP-resampling was expected to be visible in every precipitation class. However, the CP-resampling did only increase the variability for the lower intensities. A possible explanation for this outcome is that the CP-sequence used for the generation with the same CP-sequence includes more wet CPs. No investigation has been carried out concerning how the CP-sequence used in the generation with the same CP-sequence is related to the other CP-sequences used in the resampling. The CP-sequence used in the generation with the same CP-sequence could include more wet years and higher extremes and that will affect the frequency distribution for the higher precipitation intensities.

Further investigations in cooperation with IWS are necessary to investigate this outcome. In future studies, it would be preferable if the frequency of extremely wet and dry CPs could be investigated for each CP-sequence. Thus, the CP-sequence representing the median should be chosen as the CP-sequence for the generation with the same CP-sequence.

When investigating the variability within the daily absolute frequencies for the future, the results were not consistent with expectations. An increase in variability in comparison to the past was expected. However, the results show a decrease in variability in comparison to the past scenario. A decrease in variability in the future has been visible in the box-and-whisker plot analysis as well. A reason for this outcome may be that there is not enough freedom in the optimization algorithm. Some parameters describing the future precipitation may be in conflict with each other, resulting in less variability in the generation. However, this is only a hypothesis and future investigations with the developers of the NiedSim-Klima generator at the IWS are necessary.

5.3 Scatter plot

An increase in variability due to the resampling of the CP-sequence in the correlation between the yearly overflow volume and the overflow duration for both the past and the future was visible. However, the results were only visibly estimated and a more mathematical approach is necessary.

5.4 Climate change

For most of the precipitation and overflow parameters, the results due to climate change were consistent with the trends of previous studies and simulations. For the precipitation parameters, the maximum values did not act as expected. This may also be due to the fact that there is not enough freedom in the optimization algorithm. However, future investigations with the developers of the NiedSim-Klima generator at the IWS are necessary.

5.5 Outlook

In this study, the mean of the 10-year period of each precipitation parameter has been used in the analysis. Through this method, variability was lost. The reason for this choice in method is that the variability within the realizations was investigated. However, for future studies, it may be a good idea to investigate the variability between the years to account for the total variability.

For future studies, it would be preferable to investigate more than one station in order to cover different hydrological conditions. The variability due to the stochastic- and the climatic effect investigated in this study are represented by the hydrological conditions in Holzgerlingen, and the results may look different for other places in Baden-Württemberg.

In this study, a similar frequency distribution analysis for the urban drainage study as for the precipitation would have been preferable, but were not realistic to carry out due to the limited time-frame. Thus, it is suggested for future investigations. Additionally, the overflow volume within certain thresholds would be calculated to form the absolute frequency distribution for the urban drainage. When comparing the absolute frequencies in the overflow volume between the **No CP res** and the **CP res**, the variability due to the resampling of the CP-sequence could be determined. The duration of the overflow event is not necessary to investigate as the duration of an event is controlled by the autocorrelation and is only influenced a little by the CP-resampling.

A frequency distribution as well as a box-and-whisker plot analysis considering precipitation events would also be suggested for the future. In this way, the variability in the precipitation events causing an overflow could also be determined.

For future investigations, the use of the scatter plot analysis would be preferable. A more mathematically correct method would be necessary, and a thorough investigation of correlated parameters has to be carried out. The scatter plots would preferably include event specific parameters for both urban drainage and precipitation. Even a correlation between precipitation and overflow parameters could give indications on the variability and its spread.

6 Bibliography

- Auer, I et al (2007) Histalp-historical instrumental climatological surface time-series of greater alpine region. *International Journal of Climatology*, 27(1), P 17-46
- Bárdossy, A., Duckstein, L. & Bogardi, I (1995). Fuzzy ruled-based classification of atmospheric circulation patterns. *International Journal of climatology* 15, P.1087-1097
- Bárdossy, A. (1998). Generating precipitation time series using simulated annealing. *Water Resources Research* 34, 7, P.1737-1744
- Beck, F. & Bárdossy, A. (2011). NiedSim-Klima: Generating Rainfall Time-Series of High Temporal Resolution under Future Climate Conditions. *Geophysical Research Abstracts*, 13
- Beck, F. & Bárdossy, A. (2013). Projecting Hourly precipitation Sums in the Future by Indirect GCM Downscaling based on Atmospheric Circulation and Temperature., Submitted to *Advances in Water Resources*
- Beck, F (2012). Generation of Spatially Correlated Synthetic Rainfall Time Series in High Temporal Resolution – A Data Driven Approach. Stuttgart, Germany: Stuttgart University. (Dissertation at the Faculty of Civil and Environmental Engineering)
- Bendel, D., Beck, F. & Dittmer, U. (2013). Modelling climate change impacts on combined sewer overflow using synthetic precipitation time-series. *Water Science & Technology*
- Butler, D. & Davies, J.W. (2010). *Urban Drainage*. 3 ed. London, United Kingdom: Spon Press
- German Association for the Water Environment (1992). *ATV-A 128E Standards for the Dimensioning and Design of Stormwater Structures in Combined Sewers*. Hennef, Germany: GFA Gesellschaft zur Förderung der Abwassertechnik.
- Ghil, M. (2002). Natural Climate Variability. *The Earth system: physical and chemical dimensions of global environmental change* 1, P. 544–549. Chichester, United Kingdom: John Wiley & Sons, Ltd
- IPCC (2007) *Fourth Assessment Report: Climate Change 2007: The AR4 Synthesis Report*. Geneva, Switzerland: IPCC

- ITWH (2009). Kontinuierliche Simulation zur Bemessung von Speicherbauwerken in urban Entwässerungssystemen – KOSIM 7.3 (Continues Simulation for the assessment of storage structures in urban drainage systems – KOSIM 7.3). Hannover, Germany: Institute für technisch-wissenschaftliche Hydrologie GmbH ITWH (Hrsg.)
- Massart, D.L, Smeyers-Verbeke, J., Capron, X., Schlesier, K. (2005). Practical Data Handling – Visual Presentation of Data by Means of Box Plots. LC CG Europe 18, 4, P.215-218
- Peltier, J. (2011). Excel Box-and-whisker Diagrams (Box Plots). Peltier Tech Blog – Peltier Tech Excel Charts and Programming. Peltier Technical Services Inc. 7th of June 2011
- Trenberth, K.E. (1999). Conceptual framework for changes of extremes of the hydrological cycle with climate change. *Climate change*, 42, P. 327-339
- Wischet, W & Endlicher, W. (2008). Einführung in die allgemeine Klimatologie. Gebrüder Borntraeger Verlagsbuchhandlung, 7 ed.

6.1 Figures

- Figure 2.1:** Butler, D. & Davies, J.W. (2010). *Urban Drainage*. 3 ed. London, United Kingdom: Spon Press
- Figure 2.2:** Butler, D. & Davies, J.W. (2010). *Urban Drainage*. 3 ed. London, United Kingdom: Spon Press
- Figure 2.3:** Baden-Württemberg Studyguide (2013). Map of Baden-Württemberg [Electronic] Available at: <http://www.bw-studyguide.de/home/state/map2/page.html>
- Figure 2.4:** Beck, F (2012). *Generation of Spatially Correlated Synthetic Rainfall Time Series in High Temporal Resolution – A Data Driven Approach*. Stuttgart, Germany: Stuttgart University. (Dissertation at the Faculty of Civil and Environmental Engineering)
- Figure 2.5:** Bendel, D., Beck, F. & Dittmer, U. (2013). *Modelling climate change impacts on combined sewer overflow using synthetic precipitation time-series*. Water Science & Technology
- Figure 3.1:** © Löfvendahl, 2013
- Figure 3.2:** © Löfvendahl, 2013
- Figure 3.3:** © Löfvendahl, 2013
- Figure 3.4:** Beck, F (2012). *Generation of Spatially Correlated Synthetic Rainfall Time Series in High Temporal Resolution – A Data Driven Approach*. Stuttgart, Germany: Stuttgart University. (Dissertation at the Faculty of Civil and Environmental Engineering)
- Figure 3.5:** © Löfvendahl, 2013
- Figure 3.6:** Bendel, D., Beck, F. & Dittmer, U. (2013). *Modelling climate change impacts on combined sewer overflow using synthetic precipitation time-series*. Water Science & Technology
- Figure 3.7:** © Löfvendahl, 2013

Figure 3.8: SAS/STAT(R) 9.2 User's Guide, Second Edition (2013) [Electronic] Available at:

<http://support.sas.com/documentation/cdl/en/statug/63033/HTML/default/images/skeletal.png>

Figure 3.9: Wikipedia (2011). Box Plot [Electronic] Available at: http://en.wikipedia.org/wiki/Box_plot

Figure 3.10: © Löfvendahl, 2013

Figure 3.11: © Löfvendahl, 2013

Figure 7.1: © Löfvendahl, 2013

6.2 Tables

Table 7.1: © Löfvendahl, 2013

Table 7.2: © Löfvendahl, 2013

Table 7.3: © Löfvendahl, 2013

7 Annex

7.1 Constructing box-and-whisker plots in Excel

Microsoft Excel has been used to create the box-and-whisker plots analyzed in this study. Excel has been chosen because of its simplicity and compatibility with the Visual Basics script written for the purpose of handling the data in this study.

However, Microsoft Excel does not have a predefined box-and-whiskers diagram to directly apply and visualize the data. Nevertheless, a box-and-whisker plot can be constructed using the Excel functions *Stacked Column Chart* and *Error Bars*.

The parameters analyzed are simple descriptive statistics for precipitation, as mentioned above. For each realization, the mean of the 10-year time period for the investigated parameter has been used as input data. This results in ten values for each of the four generation combinations, see Table 7.1 below.

Table 7.1. Example of the set up of the table to determine the variability within the 10 realizations by box-and-whisker plots (Löfvendahl, 2013)

	A	B	C	D	E	F	G	H	I	J	K
1	Mean 60min	Run 1	Run 2	Run 3	Run 4	Run 5	Run 6	Run 7	Run 8	Run 9	Run 10
2	No resampling klim	0,547	0,568	0,550	0,553	0,555	0,553	0,566	0,546	0,530	0,561
3	Resampling klim	0,541	0,557	0,536	0,539	0,551	0,539	0,582	0,561	0,537	0,562
4	No resampling dist	0,600	0,573	0,580	0,568	0,589	0,576	0,571	0,607	0,593	0,596
5	Resampling dist	0,553	0,579	0,622	0,565	0,596	0,570	0,571	0,573	0,565	0,603

The method described by Jon Peltier on the Peltier Tech Blog in June 2011, has been used to construct the box-and-whisker plots in this study (Peltier, 2011).

First, the necessary statistics needed to construct the box-and-whisker plots are calculated for each generation combination, see Table 7.2. The statistics calculated are the arithmetic mean, the minimum and maximum value, and the 25 %- and 75 % percentiles. The count is the number of realizations in each generation combination. The mean, median, minimum, and maximum values are common statistics of a population and do not need any further explanation. The QUANTIL function calculates the k-percentile for a population. As the 25 % and 75 % percentile represents the interquartile range, k is set to 0.25 and 0.75 respectively. The formulas are in German as the language setting in the Excel program is German.

Table 7.2. Example of the statistics and their respective formulas used to calculate and construct the box-and-whisker plots. (Löfvendahl, 2013)

	A	B	C	D	E	F
12	k1	0,25				
13	k3	0,75				
14		No res klim	Res klim	No res dist	Res dist	Formulas column B
15	Count	10	10	10	10	=ANZAHL(B2:K2)
16	Mean	0,553	0,551	0,585	0,580	=MITTELWERT(B2:K2)
17	Min	0,530	0,536	0,568	0,553	=MIN(B2:K2)
18	Q1	0,548	0,539	0,574	0,567	=QUANTIL(B2:K2; \$B\$12)
19	Median	0,553	0,546	0,585	0,572	=MEDIAN(B2:K2)
20	Q3	0,560	0,560	0,595	0,592	=QUANTIL(B2:K2; \$B\$13)
21	Max	0,568	0,582	0,607	0,622	=MAX(B2:K2)

Additionally, the values used in constructing the box-and-whisker plots are calculated, see Table 7.3. The height of the bottom bar is the 25 % percentile value as this is where the lower-quartile box begins. The second-quartile box is therefore the difference between the median and the 25 % percentile. Likewise, the 3Q Box, the upper quartile, is the difference between the 75 % percentile and median. The lower whisker is the difference between the 25 % percentile and the minimum value while the upper whisker is the difference between the maximum value and the 75 % percentile.

Table 7.3. Example of the input values calculated to construct the box-and-whisker plots (Löfvendahl, 2013)

	A	B	C	D	E	F
12	k1	0,25				
13	k3	0,75				
14		No res klim	Res klim	No res dist	Res dist	Formulas column B
15	Count	10	10	10	10	=ANZAHL(B2:K2)
16	Mean	0,553	0,551	0,585	0,580	=MITTELWERT(B2:K2)
17	Min	0,530	0,536	0,568	0,553	=MIN(B2:K2)
18	Q1	0,548	0,539	0,574	0,567	=QUANTIL(B2:K2; \$B\$12)
19	Median	0,553	0,546	0,585	0,572	=MEDIAN(B2:K2)
20	Q3	0,560	0,560	0,595	0,592	=QUANTIL(B2:K2; \$B\$13)
21	Max	0,568	0,582	0,607	0,622	=MAX(B2:K2)
22	Bottom	0,548	0,539	0,574	0,567	=B20
23	2Q Box	0,0053	0,0076	0,0108	0,0055	=B21-B20
24	3Q Box	0,0069	0,0137	0,0107	0,0196	=B22-B21
25	Whisker-	0,0174	0,0022	0,0057	0,0138	=B20-B19
26	Whisker+	0,0082	0,0224	0,0118	0,0301	=B23-B22

Finally, the box-and-whisker plots can be constructed by using the Excel functions *Stacked Column Chart* and *Error Bars*. The data yields four different categories representing the four generation types. The bottom, 2Q Box and 3Q Box are representing the columns stacked on top of each other in each category.

The whiskers are added to each box plot by adding error bars from the 2Q Box, lower whisker, and the 3Q Box, upper whisker. The bottom column is “removed” by changing its lines and filling color to transparent. The mean is added in the box-and-whisker plots by copying the mean into the chart as a line with markers. The line can then be removed and the mean will be represented as markers in the box-and-whisker plots. The final result is presented in Figure 7.1 below.

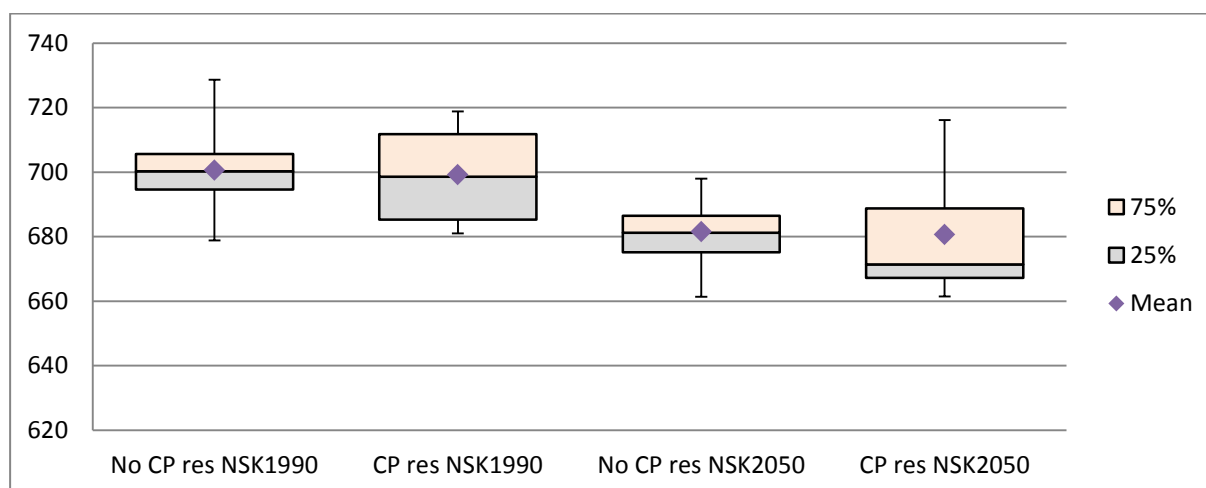


Figure 7.1. An example of a complete box-and-whisker plot used in this study (Löfvendahl, 2013).